The splicing factor kinase, SR protein kinase 1 (SRPK1) is essential for late events in the human papillomavirus life cycle.

Arwa A. A. Faizo[1], Claire Bellward[2], Hegel R. Hernandez-Lopez[3], Andrew Stevenson, Quan Gu, and Sheila V. Graham[4].

MRC-University of Glasgow Centre for Virus Research, School of Infection and Immunity, College of Medical, Veterinary and Life Sciences, University of Glasgow. Glasgow, Scotland UK.

[1]Current address:
Special Infectious Agents Unit, King Fahd Medical Research Center, King Abdulaziz University, P.O. Box 128442, Jeddah 21362, Saudi Arabia and Department of Medical Laboratory Technology, Faculty of Applied Medical Sciences, King Abdulaziz University, P.O. Box 80324, Jeddah 21589, Saudi Arabia.

[2]Current address:
Fios Genomics, BioCube 1, 13 Little France Road, Edinburgh BioQuarter, Edinburgh EH16 4UX, Scotland.

[3]Current address:
Illumina Belgium, Schaliënhoevedreef 20H, 2800 Mechelen, Belgium.

[4]Corresponding author:
Address: Botham Building, Garscube Estate, University of Glasgow, Glasgow G61 1QH, Scotland, UK.
Tel: +44 141 330 6256
E-mail: Sheila.Graham@glasgow.ac.uk

Short title: SRPIN340 inhibits late events in the HPV16 life cycle.

ABSTRACT

Human papillomaviruses (HPV) infect epithelial causing benign lesions. However, the so-called “high risk” HPVs that infect the anogenital regions and the oropharynx can cause precancerous lesions that can progress to malignant tumours. Understanding the HPV life cycle is important to the discovery of novel antiviral therapies. HPV uses cellular splicing for the production of the full suite of viral mRNAs. Members of the serine/arginine rich (SR) protein family can positively regulate splicing. SR protein activity and cellular location is regulated by kinases through phosphorylation of their serine-arginine domains. SR protein kinase 1 (SRPK1) phosphorylates SR proteins to licence their nuclear entry and can promote nuclear splicing in conjunction with another SR protein kinase, Clk1. SRPIN340 is a specific SRPK1 inhibitor that has been reported to inhibit replication of HCV, Sindbis virus and HIV. Using organotypic raft cultures supporting the HPV16 life cycle, we show that SRPIN340 inhibits the expression of the viral replication and transcription factor, E2. Drug-mediated loss of E2 is specifically associated with inhibition of late gene expression since early gene expression is unaffected. RNA sequencing revealed that SRPIN340 treatment resulted in many gene expression changes opposite to those induced by HPV16 infection. In particular, the loss of epithelial barrier structure and immune function was restored. SRPIN340 treatment resulted in changes in alternative splicing of 935 RNAs and pathway analysis showed a predominance of changes to RNAs encoding proteins involved in chromatin conformation, DNA repair and RNA processing. SRPIN340 treatment was not associated with changes in proliferation or differentiation of keratinocytes. Collectively, these results provide evidence that SRPK1 is a host factor that is essential for HPV16 replication and therefore, targeting this factor, or the phosphorylation events it mediates, could be considered as a therapeutic strategy for HPV16 infection.

AUTHOR SUMMARY

Human papillomavirus (HPV) can cause precancerous and cancerous tumours of the anogenital region, for example, the cervix. HPV infects epithelial cells and utilizes the host cell

gene expression machinery to produce its own proteins. Splicing is a key mechanism used by HPV to synthesise messenger RNAs that encode the viral proteins. Splicing is positively controlled by SR proteins which require to be phosphorylated by SR protein kinase (SRPK) to enter the nucleus and regulate splicing. SRPIN340 is a specific inhibitor of SRPK. SRPIN340 treatment of HPV16-infected epithelial cells resulted in loss of expression of the viral replication and transcription factor, E2 and abrogation of late events in the viral life cycle. SRPIN340 treatment counteracted some gene expression changes to the epithelium known to be cause by HPV infection. These data suggest that SRPK1 is essential for the HPV life cycle and that it could be a potential anti-viral target.

Key words: Human papillomavirus; SR protein kinase; splicing; drug therapy.

68 **INTRODUCTION**

69 Human papillomaviruses (HPVs) are sexually transmitted and infect cutaneous and mucosal
70 epithelia to cause benign lesions or warts [1]. Most HPV infections are asymptomatic and are
71 eventually cleared by the host immune system [2]. However, persistent infection with one of
72 the so-called high-risk HPVs (HR-HPVs), primarily HPV16 and HPV18, can cause lesions in
73 oropharyngeal and anogenital mucosa which may progress to cancer. Globally, HPV16 and
74 HPV18 infections account for up to 70% of cervical cancers, with HPV also linked to cancers
75 in the head and neck, particularly in the oropharynx [3]. Vaccination against the most prevalent
76 HR-HPVs has been delivered over almost the last two decades to young people prior to sexual
77 debut [4]. However, the vaccines are prophylactic which means that there are several
78 decades-worth of infected individuals who have not been vaccinated or have declined
79 vaccination. Therefore, development of antivirals against HR-HPV infection is essential.
80 Understanding viral gene regulation is important to this aim.

81

82 The HPV life cycle is intimately linked to differentiation of the epithelium it infects and is tightly
83 regulated by virus-host interactions [5]. HPV early proteins E1 and E2 control viral replication.
84 They are first expressed in basal epithelial cells to establish infection, then are expressed later
85 in the upper epithelial layers to enable vegetative viral genome replication prior to virion
86 formation [6]. E2 is also the viral transcription factor. Viral E6 and E7 proteins, are expressed
87 throughout the life cycle to activate the cell cycle and suppress differentiation of suprabasal
88 epithelial cells while stopping the apoptotic response by degrading p53 [7, 8]. The most
89 abundant late protein is E4, which can alter keratinocyte filaments to facilitate virus replication
90 and egress [9]. The final event in the HPV life cycle is expression of the capsid proteins L1
91 and L2. Capsid protein expression is restricted to the outermost epithelial layers, an immune-
92 privileged site, to avoid activation of the host immune response [5].

93

94 Constitutive and alternative splicing, directed by RNA Polymerase II (RNAPII) transcription
95 and the splicesome, are essential host cell mechanisms for production of multiple mature

96 mRNAs from a single gene. Constitutive and alternative splicing is regulated and enhanced
97 by serine-arginine-rich splicing factors (SRSFs) through their roles in splice site selection,
98 exon definition, spliceosome recruitment and stabilisation [10, 11]. They can bind to exonic
99 and intronic sequence enhancers (ESEs/ISEs) to promote splicing at specific sites. The
100 classical SRSFs include SRSF1-9 which all have a common structure composed of an N-
101 terminal RNA recognition motif (RRM), a C-terminal domain, which functions in spliceosome
102 regulation and protein interactions, and a serine-arginine-rich (RS) domain [11]. The RS
103 domain is subject to phosphorylation by kinases including serine/arginine protein kinase 1
104 (SRPK1) and CDK-like kinase 1 (Clk1) [12, 13]. This post-translational modification regulates
105 both the function and subcellular localisation of SRSFs [14, 15]. SRPK1 is normally present
106 in the cytoplasm of cells where it phosphorylates newly synthesised SRSFs, to licence their
107 entry into the nucleus [16]. In the nucleus, SRPK1 interacts with Clk1 to promote splicing [13].
108
109 HPV gene expression is regulated at the transcriptional and post-transcriptional levels [17].
110 Production of viral proteins occurs from multiple alternatively spliced mRNAs [18]. HPV utilizes
111 the host cell splicing machinery, including SR proteins, for viral protein expression, but also
112 controls host cell splicing. For example, the E2 transcription factor of the HR-HPVs, HPV16
113 and HPV31, transcriptionally activates the promoters of the genes encoding SRSFs 1, 2 and
114 3, up-regulates SRPK1, and can bind SRSFs [19-21].
115
116 SRPIN340 is a specific inhibitor of SRPK1 through binding to the enzyme's active site [22,
117 23]. SRPIN340 has been shown to have anti-angiogenesis properties by inhibiting VEGF
118 splicing and has been suggested as a potential therapy against exudative age-related macular
119 degeneration and diabetic nephropathy, among other diseases [22, 23]. SRPIN340 has been
120 shown to inhibit replication of HIV, Sindbis virus and hepatitis C virus [24, 25]. SRPK1 and SR
121 proteins are essential factors for the life cycle of other viruses such as herpes simplex virus
122 type 1 (HSV1) [26] and hepatitis B virus (HBV) [27] suggesting that drugs to inhibit SRPK1
123 could have a general activity against a range of viruses.

124 We tested the hypothesis that SRPIN340 could inhibit the HPV life cycle through regulating
125 the SR proteins known to be required for HPV mRNA expression [28, 29]. We focused on
126 HPV16 as the most prevalent HPV genotype. We assessed the effect of SRPIN340 on viral
127 protein expression (E2, E4, E6, E7 and L1), and cellular SR proteins (SRSF1-3). We also
128 investigated whether SRPIN340 is associated with toxicity to the host cells in three-
129 dimensional raft cultures. Our results demonstrate that inhibiting SRPK1 using SRPIN340 can
130 inhibit the expression of the HPV E2 replication/transcription factor, and lead to loss of HPV
131 late gene expression. Early gene expression was unaffected. No significant change to
132 epithelial growth or differentiation or to cellular proliferation or viability was detected. RNA
133 sequencing revealed that SRPIN340 induced some changes to keratinocyte differentiation,
134 and to the epithelial barrier, opposite to those caused by HPV infection.
135

136 **RESULTS**

137 Work by others has shown inhibition of replication of HIV, Sindbis virus and hepatitis C virus
138 by the SRPK1 inhibitor SRPIN340 [24, 25]. Following on from our previous findings that
139 HPV16 E2 up-regulated SRPK1 during the HPV life cycle [20], we were interested in
140 determining if SRPIN340 could act as an antiviral against HPV. First, we wanted to check if
141 there was any effect of the drug on the growth or morphology of 3D raft tissues supporting
142 HPV infection. We grew raft tissues using HPV16-infected keratinocytes (NIKS16 cells: normal
143 immortalised keratinocytes stably transfected with episomal HPV16 genomes [30, 31]
144 (Supplementary Fig 1)). HPV16 was chosen as the primary focus due to its high prevalence
145 among high-risk HPV types associated with anogenital and oropharyngeal cancers. We chose
146 to test concentrations of the drug at 10 μM or 50 μM since these concentrations had been
147 optimised in previous virus replication studies [24, 25]. Preliminary titration assays confirmed
148 that these concentrations were optimal for effective inhibition of SRPK1 without compromising
149 cell viability in keratinocyte monolayer cultures. Compared to the drug vehicle DMSO, the
150 addition of SRPIN340 in the culture medium after 12 days of tissue growth at either 10 μM or
151 50 μM, and applied for 48 hours, caused disordered growth of the raft tissues (Supplementary
152 Fig 2A). To minimize the effect of the drug on tissue morphology we developed a method of
153 applying the drug to the upper surface of the tissues in a 50 μl droplet also for the last 48 hours
154 of a 14-day growth period. This volume was chosen because it covered the surface of the
155 tissue without reaching the edge. In contrast to the significant disruption to tissue morphology
156 when SRPIN340 was added to the culture media, there was no observable difference in
157 morphology between DMSO or 10 μM SRPIN340-treated tissues when the drug was applied
158 to the top of the tissues (Supplementary Fig 2B). Some disruption of the upper epithelial layers
159 was observed when the drug was applied at 50 μM (Supplementary Fig 2B).

160

161 To test whether SRPIN340 could enter the epithelium upon topical application we applied the
162 fluorophore Alexa 488 in a 50 μl droplet to the top of the raft tissues. This molecule has a
163 similar chemical structure to SRPIN340, which has a molecular weight of 349 Daltons. Alexa

164 Fluor 488 with a molecular weight of 570 Daltons is known to be transmitted between cells by
165 gap junctions, which permit intercellular spread of molecules >1 kDa in size [32]. As a control,
166 topical application of DMSO produced no autofluorescence (Supplementary Fig 2C). Topical
167 application of Alexa 488 revealed penetration down to the basal layers of the tissues and
168 fluorescence was distributed into all the cell layers of the epithelium (Supplementary Fig 2D).
169 This suggests that SRPIN340, which is a smaller molecule than Alexa Fluor 488, could travel
170 through gap junctions throughout the epithelium.
171
172 **SRPIN340 treatment leads to reduced phosphorylation and relocation to the cytoplasm**
173 **of shuttling SR proteins in keratinocytes.**
174 To assess whether topically applied SRPIN340 had biochemical effects in HPV16-positive
175 cells, we quantified the levels of SRSF1 and 3, which are phosphorylated by SRPK1 [10], in
176 NIKS16 tissues grown for 12 days and then topically treated for 48 hours with either DMSO
177 or SRPIN340 and compared this with a control SR protein SRSF2, which is a poor substrate
178 of SRPK1. Using a phospho-specific antibody (Mab104) we found that levels of
179 phosphorylated SRSF1 and SRSF3 were reduced upon drug treatment (Fig 1A, C), while
180 levels of SRSF2 did not change significantly, as expected (Fig 1B). Next, we analysed the
181 effect of SRPIN340 on the subcellular location of SRSF1 and SRSF3, whose import into the
182 nucleus is controlled by phosphorylation by SRPK1, and SRSF2, which is mostly confined to
183 the nucleus [10, 11]. Compared to a mainly nuclear location in DMSO-treated NIKS16 cells,
184 SRSF1 and SRSF3 were found in the cytoplasm in SRPIN340-treated NIKS16 cells (Fig 1D,
185 F). In contrast, SRSF2 maintained a nuclear location in both DMSO and SRPIN340-treated
186 cells (Fig 1E). These data confirm efficacy of SRPIN340 in inhibiting the activity of SRPK1 in
187 in HPV16-positive keratinocytes.
188
189 **SRPIN340 treatment does not change E6E7 oncoprotein expression or activity.**
190 First, as a measure of HPV early gene expression, we investigated if SRPIN340 as an anti-
191 splicing drug affected the expression of the alternatively spliced mRNAs encoding the HPV16

192 E6 and E7 oncoproteins (Fig 2A). For these experiments we used NIKS16 cells grown in
193 monolayer culture. End-point PCR analysis showed that the four main splice isoforms of E6E7
194 mRNAs were present, and their levels were unchanged in the presence of the drug (Fig 2B).
195 Levels of E7 and E6 proteins in NIKS16 cells were much lower than their levels in HeLa cells
196 as a control for oncoprotein detection. Importantly, there was no detectable difference in levels
197 of E6 (Fig 2C, D) or E7 proteins (Fig 2E, F) upon drug treatment. Expression levels of the E6
198 degradation target protein, p53 and the E7 target, Rb were also unaffected (Fig 2G, H).
199
200 **SRPIN340 inhibits the expression of the viral E2 replication/transcription factor.**
201 Next, we investigated the expression of viral late mRNAs using NIKS16 cells grown and
202 differentiated in monolayer culture to express viral late proteins (Supplementary Fig 1B).
203 Expression of the major late HPV16 spliced transcript, E1^E4^L1 and the L2L1 portion of the
204 readthrough transcript E1^E4, E5, L2, L1 (Supplementary Fig 3A) was not altered by
205 SRPIN340 in differentiated NIKS16 cells (Supplementary Fig 3B, C). However, expression of
206 the major mRNA encoding the viral E2 replication/transcription factor [33] (Fig 3A) was
207 inhibited when differentiated NIKS16 cells were treated with the drug (Fig 3B, lane 3).
208 Treatment with DMSO (Fig 3B, lane 1) or with SRPIN349, a SRPIN340 derivative which does
209 not inhibit the kinase activity of SRPK1 [25] (Fig 3B, lane 2), did not affect the expression of
210 the E2 mRNA. Western blot analysis of SRPIN340-treated NIKS16 cells differentiated in
211 monolayer culture revealed that drug treatment inhibited expression of the E2 protein (Fig 3C).
212 Detection of involucrin revealed that the cells were differentiated (see also Supplementary Fig
213 1B). Quantification of three separate experiments showed a statistically significant difference
214 in E2 levels upon drug treatment (Fig 3D). HPV-negative NIKS cell extract was included in the
215 western blot as a control for the specificity of the E2 antibody. E2 levels were also significantly
216 reduced in drug-treated NIKS16 raft tissues compared to DMSO-treated controls (Fig 3E).
217 Confocal immunofluorescence microscopy confirmed that while E2 expression was detected
218 in the upper layers of NIKS16 3D raft cultures treated with the drug vehicle DMSO, very little
219 E2 was present in drug-treated tissues (Fig 3F). Taken together, these data indicate that

220 SRPIN340 treatment is associated with reduced expression of the alternative spliced HPV16
221 E2 mRNA, suggesting that SRPK1 kinase activity is important for its expression.
222
223 **SRPIN340 inhibits late events in the HPV16 life cycle.**
224 Loss of the viral replication and transcription factor E2 could result in abrogation of late events
225 in the viral life cycle [6]. We tested this by examining the expression of the major capsid protein
226 L1. Expression of L1 was significantly reduced by SRPIN340 treatment in differentiated
227 NIKS16 cells grown in monolayer culture (Fig 4A, B). Once again, HPV-negative NIKS cell
228 extract was included in the western blot as a control for the specificity of the L1 antibody.
229 Detection of involucrin revealed that the cells were differentiated. A reduction in L1 protein
230 expression was also found in NIKS16 raft tissues grown for 12 days and then topically treated
231 with DMSO or SRPIN340 for 48 hours (Fig 4C, D). E4 is the most abundantly expressed late
232 viral protein. Although antibodies against E4 work poorly in western blot, the E4 B11 antibody
233 can be used successfully in confocal immunofluorescence microscopy. We performed
234 immunofluorescence staining with E4 (Fig 4E) and L1 (Fig 4F) antibodies on sections of
235 DMSO-treated or SRPIN340-treated NIKS16 raft tissues to confirm drug-induced restriction
236 of late events in viral replication. There was a substantial loss of both these late proteins in 3D
237 raft tissues upon drug treatment suggesting that SRPIN340 treatment is associated with
238 inhibition of the late phase of the viral life cycle, potentially due to SRPK1 inhibition.
239
240 **SRPIN340 results in significant changes in gene expression in NIKS16 cells opposite**
241 **to those induced by HPV16 infection.**
242 SRPK1 inhibition can change how SR proteins regulate splicing, leading to changes in the
243 cellular transcriptome. To our knowledge, SRPIN340-induced changes to cellular transcription
244 in keratinocytes have never been reported. In addition, HPV E2 is known to regulate the
245 expression of many cellular genes [34], including SR proteins [19], so loss of E2 expression
246 could contribute to SRPIN340-induced gene expression changes in HPV-infected cells. We
247 carried out RNA sequencing (RNA-Seq) to compare gene expression profiles of SRPIN340-

248 treated to DMSO-treated NIKS16 cells grown in monolayer culture in three replicates of each
249 condition (Fig 5A). Read coverage of the human and viral genomes was not altered by drug
250 treatment (Table 1). However, drug treatment caused a significant change in cellular gene
251 expression (Fig 5A). A total of 342 cellular transcripts were up-regulated, while 241 transcripts
252 were down-regulated (Supplementary Table 1) with a fold change of >log 2.0, Q-value <0.05.
253 Table 2 shows the top 20 up-and down-regulated genes. Ingenuity pathway analysis showed
254 that genes whose expression was up-regulated by SRPIN340 treatment in HPV-infected cells
255 were involved in keratinocyte differentiation, metabolism, immune response and the epithelial
256 barrier (Fig 5B). Down-regulated pathways included aspects of morphogenesis and cell
257 motility, while cell adhesion and the immune system were upregulated, which is consistent
258 with the antiangiogenic activity of the drug (Fig 5C) [22].
259
260 We compared the gene expression profiles of SRPIN340-treated NIKS16 cells to HPV16-
261 induced gene expression changes that we identified in a previously acquired dataset
262 comparing compared gene expression changes between uninfected NIKS cells (baseline) and
263 HPV16-infected NIKS16 cells [35]. For this analysis, and to capture the maximum number of
264 genes in common, we focused on genes that exhibited a fold change >log 1.5. Analysis of
265 these changes revealed 91 genes whose expression was altered in both conditions. One
266 important known change to the epithelium caused by HPV16 infection is an abrogation of
267 keratinocyte differentiation and loss of both structural and immune aspects of the epithelial
268 barrier. Comparison of the datasets showed that SRPIN340 treatment led to up-regulation of
269 keratinocyte differentiation genes and epithelial barrier-associated genes that were previously
270 shown to be down-regulated by HPV16 infection. Genes encoding proteins involved in
271 keratinocyte terminal differentiation such as filaggrin and keratin 10, epithelial structural barrier
272 such as loricrin, transglutaminase and repetin [36], and the immune barrier such as keratin 16
273 [37] and SPRR proteins [38] (Fig 5D), were up-regulated by drug treatment. Moreover,
274 SRPIN340 affected the expression of five genes encoding key immune regulators, including
275 the interferon response factor IRF1 (Fig 5E) which are known to be modulated by HPV16

276 infection. These findings suggest that SRPIN340 may have the potential to restore some
277 aspects of normal keratinocyte function altered by HPV16 infection.
278
279 **SRPIN340 induces alternative splicing changes related to key processes in the HPV life**
280 **cycle.**
281 RNA-Seq data from triplicate 10 μM SRPIN340-treated and DMSO-treated NIKS16 cells were
282 aligned to the human genome and subjected to alternative splicing analysis using the
283 bioinformatic tool SplAdder. 'Percentage spliced in' (PSI) values, which are calculated based
284 on the frequency of a particular exon being spliced into a specific splice isoform, were
285 calculated by SplAdder, and used as a measurement of alternative splicing events comparing
286 between SRPIN340-treated and DMSO-treated cells. Differentially spliced genes were then
287 ranked by statistical significance. SRPIN340 treatment resulted in changes in alternative
288 splicing of 935 genes (Supplementary Table 2).
289
290 To infer the biological significance of the changes to alternative splicing induced by SRPIN340
291 treatment in NIKS16 cells, the genes identified as alternatively spliced were subject to pathway
292 analysis. Over-representation analysis was performed on the 935 significantly alternatively
293 spliced genes (p-value <0.05) by Webgestalt [39]. The biological processes affected by the
294 changes in alternative splicing caused by SRPIN340 treatment included RNA splicing, as
295 expected due to the major role of SRPK1 in regulating splicing. However, splicing of transcripts
296 encoding DNA repair factors/DNA damage response was also significantly altered (Fig 5F).
297 The DNA damage response is essential for HPV replication and alternative splicing-induced
298 changes in DNA repair factors could create a cellular environment inhibitory to HPV
299 replication.
300
301 **SRPIN340 is not toxic to keratinocytes.**
302 If SRPIN340 can inhibit HPV16 replication it could have therapeutic potential. However,
303 cellular toxicity due to effects on host cell alternative splicing must be considered. We

304 examined the toxicity of SRPIN340 in uninfected NIKS and HPV-infected NIKS16
305 keratinocytes. Drug concentrations of 10 μM and 50 μM were tested over a period of 72 hours
306 using cells grown in monolayer culture. DMSO was used as the vehicle control. Cell
307 proliferation was not affected by either drug concentration in either cell line (Fig 6A, B). A small
308 decrease in proliferation of NIKS16 cells was observed at the highest drug concentration
309 following treatment for 72 hours, however, this was not statistically significant (Fig 6B). Cell
310 viability of NIKS cells was only decreased significantly at the highest drug concentration
311 following treatment for 72 hours (Fig 6C), while NIKS16 cell viability was unaffected (Fig 6D).
312 Quantification of two cell proliferation markers, Ki67 and MCM2 confirmed that there was no
313 statistically significant change in cellular proliferation upon drug treatment of either NIKS (Fig
314 6E, F) or NIKS16 cells (Fig 6G, H). These data suggest that short-term SRPIN340 treatment
315 is not toxic to HPV-negative or HPV-positive keratinocytes.
316
317

318 **DISCUSSION**

319 Here we have demonstrated that SRPK1 activity is essential for the expression of the HPV16
320 E2 replication and transcription factor. We showed that key early and late viral mRNAs were
321 synthesised in the presence of SRPIN340. Therefore, transcription of the viral genome is not
322 inhibited by drug treatment, as expected since SRPK1 is associated with post-transcriptional
323 events. Drug treatment did not affect the production of early spliced mRNAs or the late
324 unspliced read-through mRNA containing open reading frames for L2 and L1, suggesting that
325 SRPIN340 specifically inhibits alternative splicing of the E2 mRNA. It is not known which SR
326 proteins are required for E2 splicing. However, a bioinformatic tool, ESE finder [40], predicts
327 with high confidence the binding of SRSF2 and SRSF5 to a sequence 182 bases from the E2
328 splice acceptor site at nt 2709. Since the activity of SRSF2 is not affected by SRPIN340
329 treatment, this suggests that E2 alternative splicing is regulated at least in part by SRSF5.
330 Studies by others have shown that hnRNP G has an enhancing effect on splice acceptor 2709
331 by binding to a sequence between the E2 splice acceptor site and the E2 start codon [41].
332 Both splicing regulatory factors could cooperate to enhance recognition of the E2 splice site.
333

334 E2 regulates alternative splicing of cellular genes [42], which may be due to E2 activating
335 transcription of SR proteins [19]. E2 can also interact with SR proteins and inhibit splicing of
336 suboptimal introns [21]. HPV1 E2 is phosphorylated by SRPK1 [43] but although HPV16 E2
337 is subject to phosphorylation, it has not been shown to be a substrate of SRPK1, perhaps
338 because it has a short hinge region that does not contain SR repeats. However, the close
339 association of E2 with viral and cellular splicing suggests an important E2-splicing factor
340 regulatory axis in the HPV-infected cell. The requirement for SRPK1 to produce E2 protein
341 and E2 up-regulation of SRPK1 in differentiated epithelial cells [20] underscores this axis and
342 suggests that SRPK1 may be involved in promoting viral DNA replication, genome
343 transcription, and mRNA splicing.
344

345 Surprisingly, although SRPIN340 treatment did not inhibit splicing of other major HPV16
346 mRNAs, it did reduce the cellular levels of HPV major late proteins E4 and L1. This suggests
347 that SRPK1 could positively control viral late mRNA expression at a level other than splicing.
348 SRPK1 is present in the cytoplasm of differentiated HPV16-infected keratinocytes [20].
349 Therefore SRPK1 could affect mRNA stability, or translation, either directly via its interaction
350 with intracellular signalling pathways [44] or through phosphorylating SR proteins such as
351 SRSF1 involved in these processes [11]. Alternatively, loss of E2 protein, which can activate
352 L1 expression [45] and can bind both E4 and L1 proteins [46, 47], could cause a reduction in
353 levels of both proteins at a post-transcriptional level or perhaps by destabilising the proteins.
354
355 Inhibition of late events in the viral life cycle could imbalance the differentiation-dependent life
356 cycle and potentially result in persistent infection and cancer progression. However, we found
357 no evidence for any tumour-promoting activity of SRPIN340 in HPV16-positive keratinocytes,
358 since cell proliferation and viability were unchanged in the presence of the drug, and
359 repression of differentiation due to HPV infection was reversed. Importantly, we found that
360 E6E7 expression and activity were not enhanced by drug treatment.
361
362 In our RNA-Seq analyses, SRPIN340 treatment led to up-regulation of expression of
363 keratinocyte differentiation genes with 31% of drug-induced gene expression affecting
364 epithelial differentiation. Keratinocyte differentiation factors included Desmoglein 1, which
365 forms cell-cell junctions to resist mechanical stress and preserve epidermal homeostasis [48],
366 SPINK5 and Kallikrein-12 which are a serine protease inhibitor and serine protease,
367 respectively [49] and loricrin and repetin, which are components of the cornified envelope
368 together with transglutaminase 1, which is involved in its formation [36]. Expression of several
369 keratins was up-regulated as well as filaggrin which binds to keratin fibres [50]. Finally, several
370 of the SPRR proteins involved in epithelial barrier protection and immune defence were also
371 up-regulated [38]. Taken together, the up-regulation of these genes could enhance the
372 epithelial barrier thus counteracting its disruption as a result of HPV16 infection. This drug-

373 induced effect would be predicted to mechanically strengthen infected, differentiated
374 keratinocytes and inhibit HPV virion egress from the surface of the epithelium. In adddition,
375 we discovered that SRPIN340 treatment of NIKS16 cells changed alternative splicing of RNAs
376 encoding factors involved in cellular processes that are essential for HPV life cycle including
377 DNA damage repair, mRNA processing and chromatin conformation [29]. The effects of
378 SRPIN340 on host cell gene expression may provide an environment in which the host cell
379 can no longer support HPV16 replication, life cycle and transmission.
380
381 In monolayer cultures, SRPIN340 had no detectable effect on the proliferation or growth of
382 HPV negative and positive cell lines except when used at high concentration (50 μM).
383 Although there was significant disruption to 3D raft tissues when SRPIN340 was added in the
384 culture medium, there was no change in the morphology or the growth of 3D raft tissues upon
385 topical treatment with the drug at 10 μM. Although animal experiments have demonstrated
386 that systemic oral delivery of SRPIN340 (even at 2000 mg/kg rat body weight) is well tolerated
387 [24] the changes to the epithelium caused by growth of tissues in medium containing the drug
388 suggest that the drug would be best delivered topically if used as an antiviral therapy.
389 SRPIN340 has already been proposed as a topical therapy against diseases such as
390 exudative age-related macular degeneration [22] and next-generation inhibitors to be used at
391 nanomolar concentrations are being developed. VEGF mis-regulation is a key player in HPV-
392 associate cancer progression. SRPIN340 alters VEGF splicing and inhibits angiogenesis [22].
393 Therefore, although we have studied SRPIN340 activity in the HPV16 life cycle, it may have
394 potential in therapeutic treatment of HPV-associated cancers. Cancer-specific splicing can
395 lead to the expression of oncogenic protein isoforms, as has been shown for HPV-positive
396 HNSCC [51, 52], which SRPIN340 could ameliorate.
397
398 There are several limitations to this study. It is important to note that we carried out the
399 analyses in differentiated HPV16-infected, monolayer cultured cells and in differentiated raft
400 cultured tissues so we cannot make any conclusions about the effect of SRPIN340 on early

401 events in the viral life cycle or on persistently infected cells. Additionally, we did not include
402 uninfected keratinocytes treated with SRPIN340 in our transcriptome analyses. Therefore, we
403 cannot conclusively determine whether the observed gene expression and splicing changes
404 upon SRPIN340 treatment are specific to HPV16-infected cells or represent general effects
405 on keratinocytes. Moreover, it would be important in future to determine if SRPIN340 could
406 alter expression of E2 from other high-risk HPVs, or from low-risk genotypes that cause genital
407 warts, or even those HPVs such as HPV1 that cause common warts. The long-term effects of
408 SRPK1 inhibition on epithelial cell function warrant exploration, as sustained inhibition could
409 impact processes such as cellular differentiation and tissue repair. Understanding these
410 effects will be essential for developing safe and effective therapies targeting SRPK. Given that
411 SRPIN340 targets a host factor, combining it with direct-acting antivirals could yield synergistic
412 effects, enhancing antiviral efficacy while potentially lowering the risk of resistance.
413
414 **CONCLUSIONS**
415 We have identified host cell gene expression changes following SRPIN340 treatment in
416 HPV16 infected cells. The anti-viral effect of SRPIN340 may be a combination of down-
417 regulation of production of the viral replication and transcription factor E2, together with
418 changes to splicing of host cell transcripts which collectively may alter the host cell
419 environment such that it can no longer support late events in the HPV16 life cycle. The
420 inhibition of HPV16 replication by SRPIN340 suggests that SRPK1 is a host factor crucial to
421 the HPV life cycle.
422

423 **MATERIALS AND METHODS**

424 Cell Culture

425 NIKS16 cells are normal spontaneously immortalised keratinocytes which have been
426 transfected with HPV16 genomes [30, 31]. NIKS16 cells were grown in monolayer culture on
427 a feeder layer of mitomycin-C-treated J2 3T3 cells as previously described [53] and were used
428 at a maximum passage number of 15 to avoid genome integration. NIKS16 were induced to
429 differentiate by growth at a high density in the presence of 1.2mM Ca^{2+} [19]. Cells were
430 maintained in 5% CO_2 at 37°C. NIKS16 cells were treated with either DMSO or SRPIN340
431 (Sigma, UK: SML1088) dissolved in DMSO at the given concentrations on day 8 post-seeding
432 into culture plates and cells were incubated in the presence of the drug for 48 hours.

433

434 Raft cultures were established as previously described [54] by seeding NIKS16 cells onto the
435 top of collagen matrices in 24 well plates and incubated at 37°C in 5% CO_2 for 2 days in E-
436 medium until a monolayer was formed. Rafts were lifted to the air-liquid interface on a sterile
437 stainless-steel wire grid and cultured for 14 days. The E-medium was changed every other
438 day. DMSO or SRPIN340 (Sigma) dissolved in DMSO was added to the culture medium or
439 placed on top of the raft tissues in a 50 µl droplet at the described concentrations on day 12
440 following lifting to the air-liquid interface and incubated for 48 hours.

441

442 Cell growth kinetics, viability and tissue morphology

443 Formalin fixed tissue cultures were paraffin-embedded and sectioned (2.5 µm sections).
444 Sections were haematoxylin and eosin-stained and morphology was examined under an
445 Olympus Bx57 light microscope. For cell viability and estimation of cell number, cells were
446 harvested by trypsinization, diluted in 0.1% trypan blue at a ratio of 1:1, and counted using a
447 haemocytometer. The number of unstained (viable) and total number of cells were
448 determined.

449

450

451 Tissue permeability of Alexa fluor 488

452 Cell to cell gap junction connectivity and raft permeability were assessed by the ability of cells
453 to transfer the Alexa Fluor 488 dye (A10436, Invitrogen). Alexa Fluor 488 dye at 10 μM was
454 added to the top of 3D cultured tissues in a 50 μl droplet on day 12 of tissue growth and
455 allowed to spread through the tissue structure for 2 days. At day 14, tissues were fixed,
456 sectioned, counterstained with DAPI and dye spread between neighbouring cells from the top
457 to the bottom of the raft structure was visualized using a Zeiss LSM 710 confocal microscope.
458 Zen black software (Zeiss) was used for capturing images.

459

460 Southern blotting

461 DNA was isolated using the QiaAmp DNA mini kit (Qiagen, Germany) according to the
462 manufacturer's instructions then subjected to restriction enzyme digestion overnight at 37°C
463 with 25 units of enzyme per 20 μg DNA. To prepare the DNA probe, plasmid pEF-HPV16 was
464 linearised by digestion with Bam HI at 10 units per μg DNA for one hour at 37°C. The digestion
465 products were fractionated on an agarose gel and the 8 kb viral genome band was excised
466 and purified using the QIAquick gel extraction kit (Qiagen, Germany) according to the
467 manufacturer's instructions. DNA was denatured by boiling for 5 min followed by chilling on
468 ice. The denatured DNA was labelled with Biotin-16-dUTP (Roche #11093070910, Merck, UK)
469 using the random primer labelling system according to the manufacturer's protocol (Roche
470 #11004760001, Merck, UK). Restriction enzyme-digested NIKS16 DNAs and, as a size
471 control, pEF-HPV16 digested with Bam HI, were fractionated on a 0.8% agarose gel in 1 x
472 Tris borate electrophoresis buffer overnight at 20 volts. Gel treatment, DNA transfer onto
473 nitrocellulose membrane and hybridisation with the pEF-HPV16 probe was carried out exactly
474 as described in the Amersham Hybond N+ protocol (Cytiva, UK).

475

476 Western blotting

477 Cells in monolayer were scraped into NP-40 lysis buffer (50 mM Tris-HCl pH 8.0, 150 mM
478 NaCl, 0.5% (v/v) NP-40 (IGPAL CA-630)), containing PhosphoSTOP (Merck, UK catalogue #
479 04693116001) and complete miniprotease inhibitor cocktail (Merck, UK, catalogue # 200-664-
480 3). Protein extraction from raft culture was carried out by adding a small amount of liquid
481 nitrogen to the tissue and grinding to a powder in a mortar and pestle. NP-40 lysis buffer
482 containing PhosphoSTOP (Roche) and complete miniprotease inhibitor cocktail as above was
483 added to the ground tissue, mixed and collected in 0.5ml Eppendorf tubes. The insoluble
484 matrix was removed by centrifugation for 20 min at 13,000 g at 4°C. All protein concentrations
485 were determined using Bradford's assay and a NanodropTM spectrophotometer (Thermo
486 Scientific).
487
488 Protein samples were resolved by 4-12% Bis-Tris SDS-PAGE (Invitrogen, UK catalogue
489 #NP0322BOX) using 1X NuPAGE MES gel running buffer (Invitrogen, UK, catalogue #
490 NP0002). Separated proteins in the gel were electro-transferred onto nitrocellulose membrane
491 at room temperature using the iBlot™ Dry Blotting System (Invitrogen, UK). Membranes were
492 blocked in 5% foetal bovine serum (FBS) in phosphate buffered saline (PBS) for 60 min at
493 room temperature. Membranes were incubated with primary antibody diluted in PBS-T (PBS
494 with 0.1% Tween) containing 5% FBS overnight at 4°C before being washed three times with
495 PBS-T. Primary antibodies were SRSF1 (1:1000, Mab96, Thermo Fisher Scientific, catalogue
496 # 32-4500), SRSF2 (1:1000, Abcam, catalogue #Ab204916), SRSF3 (1:500, Life
497 Technologies, UK, catalogue #334200), SRPK1 (1:500, clone G211-637 BD Transduction
498 Laboratories, catalogue #611072), α-tubulin (1:5000, clone A11126, Thermo Fisher Scientific
499 catalogue # 236-10501), involucrin (1:1000 clone SY5, Merck, UK, catalogue #19018),
500 GAPDH (1:1000, Meridian Life Sciences, UK, catalogue #H86504M, clone 6C5), HPV16 E2
501 (1:500 Santa Cruz, Germany, catalogue #sc-53327, TVG271), HPV16 E6 (1:500, Santa Cruz,
502 Germany, catalogue # sc-365089), HPV16 E7 (1:500 Santa Cruz, Germany, catalogue #sc-
503 51951), HPV16 L1 (1:500 Dako, Denmark, clone K1H8), p53 (1:700, BD Pharmingen, UK,
504 catalogue #554294), Rb (1:500, Cell Signaling Technologies, Germany, catalogue #9309,

505 clone 4H1), MCM2 (1:500, Abcam, UK, catalogue #Ab133325), Ki67 (1:1000, Abcam, UK,
506 catalogue #Ab197234), keratin 10 (1:500, Abcam, UK, catalogue #Ab9025). Monoclonal
507 antibody104 (Mab104), which detects phosphorylated SR proteins, was prepared from
508 hybridoma supernatants (ATCC CRL-2067) and used neat. Secondary antibodies were diluted
509 in PBS-T containing 5% FBS and incubated with the membrane for 1h followed by three
510 washes in PBS-T, two washes in PBS, and one rinse in dH_2O. Secondary antibodies were
511 goat anti-rabbit Dylight 800 conjugate (1:2000, Thermo-Fisher, UK, catalogue #SA5-35571),
512 goat anti-mouse Dylight 800 conjugate (1:2000, Thermo-Fisher, UK, catalogue #SA5-35521)
513 and IRDye anti-mouse 800CW (1:2000, IRDye Licor Biosciences Ltd, UK, catalogue #926-
514 32210). Membranes were imaged on an Odyssey Infrared Imager (LiCOR). The intensity of
515 protein bands was quantified using Odyssey Image Studio software. Protein levels were
516 determined and normalised to the level of the endogenous control.

517 Immunofluorescence staining and confocal microscopy

518 Monolayer cultured cells were grown on coverslips until 70% confluent. Coverslips were
519 washed three times with PBS and cells were fixed in PBS containing 5% formaldehyde at
520 room temperature for 10 min. Permeabilization was carried out with PBS containing 0.5%
521 NP40 at room temperature. Coverslips were then washed three times with PBS. Blocking was
522 done in 10% filtered donkey serum in PBS for 30 min, followed by incubation with primary
523 antibodies diluted in the blocking solution for 60 min at room temperature, and then washed
524 three times with PBS followed by another wash in distilled H_2O. Primary antibodies were
525 SRSF1 (1:250, Mab96, Thermo Fisher Scientific, catalogue # 324500), SRSF2 (1:500,
526 Abcam, catalogue #Ab204916), SRSF3 (1:300, Life Technologies, UK, catalogue #334200),
527 HPV16 L1 (1:300 Dako, Denmark, clone K1H8), HPV16 E2 sheep antibody was a kind gift
528 from Prof. Jo Parish, University of Birmingham, UK and was used at a dilution of 1:300, HPV
529 E4 antibody clone B11 was a kind gift from Prof John Doorbar, University of Cambridge and
530 was used at a dilution of 1:300. DAPI and secondary antibodies were diluted in blocking
531 solution and added to the cells for 60 min, protected from light, prior to six washes in PBS

532 followed by one wash in dH_2O. Alexa fluor secondary anti-rabbit antibody 555 (1:1000,
533 Invitrogen, UK, catalogue #A-31572), Alexa fluor secondary anti-mouse antibody 488 (1:1000,
534 Invitrogen, UK, catalogue #A-21202), Alexa fluor secondary anti-sheep 488 antibody (1:1000,
535 Invitrogen, UK, catalogue #A-11-15). Coverslips were mounted on glass slides with a glycerol-
536 based mounting medium (Citifluor, AF1) and sealed with nail enamel. Samples were examined
537 using a Zeiss LSM 710 confocal microscope and Zen black software (Zeiss) was used for
538 capturing images.
539
540 Immunofluorescence staining of 3D organotypic raft culture sections was carried out on
541 paraffin embedded fixed 2.5 µm sections. Antigen retrieval of the fixed section was performed
542 by the histopathology department, Veterinary Diagnostic Services, University of Glasgow
543 using heat induced epitope retrieval (HIER) using the Menarini Access Retrieval Unit method.
544 Sample blocking, staining, and examination were conducted as described above.
545
546 RNA extraction and cDNA synthesis
547 Total mRNA extraction was performed using TRIZOL reagent (Invitrogen, UK) according to
548 the manufacturer's instructions. For cells in monolayer culture, medium was removed, and
549 cells were washed twice with PBS. Cells were lysed by scraping into 500 µl TRIZOL reagent
550 for each well of a 6 well plate. Purified RNA was dissolved in DEPC-treated H_2O and stored
551 at -20°C. SuperScript^{TM} III First-Strand synthesis system for RT-PCR (Invitrogen, UK) was
552 used for cDNA synthesis according to manufacturer's instructions using $(dT)_{20}$ primers.
553
554 End point RT-PCR
555 For a single round of amplification 500 ng of cDNA was used in a total volume reaction of 20
556 µl using 200nM primers, 200 µM dNTPs, 1.5 mM $MgCl_2$ and 2 units *Taq* polymerase
557 (Invitrogen, UK). The amplification protocol was one cycle at 94° C for 2 min followed by 35
558 cycles of 94° C for 30 sec, annealing temperature of 55 ^{o} C (E4^L1: E4 Forward primer 5'-
559 GTTGTTGCACAGAGACTCAGTGG-3' with L1 Reverse primer 5'-

560 CGTGCAACATATTCATCCGTGC-3') or annealing temperature of 57.8 °C (E6E7: E6 Forward
561 primer 5'- GAGAACTGCAATGTTTCAGGACCC-3' with E7 Reverse primer 5'-
562 GAACAGATGGGGCACACAATTCC-3') for 45 sec followed by extension of 72° C for 1 min.
563 There was a final extension cycle of 72° C for 10 min. GAPDH cDNA was amplified as an
564 internal control (Forward primer 5'-AGGAAATGAGCTTGACAAAG-3' and reverse primer 5'-
565 ACCACAGTCCATGCCATCAC-3')
566
567 Nested RT-PCR
568 Amplification of L2L1 readthrough and E2 spliced mRNAs required two rounds of
569 amplification. For L2L1, the first round of amplification used the same PCR reaction conditions
570 described above with one cycle at 94° C for 2 min followed by 35 cycles of 94° C for 30 sec,
571 annealing temperature of 57 °C for 45 sec followed by an extension of 72° C for 1 min. There
572 was a final extension cycle of 72° C for 10 min (L2 forward primer 5'-
573 ACATGCAGCCTCACCTACTT-3' with L1 reverse primer 1 5'-
574 AACACCTACACAGGCCCAAA-3'). For the second round of amplification, 1µl of the first
575 round PCR product was diluted in a total volume of 60 µl containing 200nM primers, 200 µM
576 dNTPs, 1.5 mM $MgCl_2$ and 2 units *Taq* polymerase. The PCR conditions were one cycle at
577 94°C for 2 min followed by 25 cycles of 94°C for 30 sec, annealing at 57°C for 45 sec and 72
578 °C extension for 1 min. This was followed with a final extension of 72 °C extension for 10 min
579 (L2 forward primer 5'-ACATGCAGCCTCACCTACTT-3' with L1 reverse primer 2 5'-
580 TGTCCAACTGCAAGTAGTCTGGATGTTCCT-3'). For E2 cDNA the conditions for the first
581 round of amplification were the same as for L2L1 cDNA except using E1 Forward primer 5'-
582 ATCTACCATGGCTGATCCTGC-3' and E2 Reverse primer 5'-
583 GCAGTGAGGATTGGAGCACTGTC-3'. The conditions for the second round of amplification
584 were the same as for L2L1 cDNA except that the annealing temperature was 63.2 °C for 35
585 cycles of amplification using E1^E2 cross splice Forward primer 5'-
586 TGGCTGATCCTGCAGATTC-3' and E2 Reverse primer 5'-
587 CTTCGGTGCCCAAGGCGACGGCTTTGGTAT-3'. 10 µl of the final PCR products were

588 fractionated on a 6% acrylamide gel. Electrophoresis was performed at 100 V and the gel
589 was stained with 0.5 µg/ml EtBr for 15 min. PCR products were visualized under UV.
590

591 Statistical analysis

592 Microsoft Excel software was used for plotting the data and calculating mean, standard
593 deviations (SD), and p-values. Statistical significance was determined by students t-test with
594 $p \leq 0.05$ considered significant. All experiments were performed at least three times.
595

596 Next Generation Sequencing

597 RNA was prepared using the Qiagen RNeasy kit from monolayer cultured NIKS16 cells grown
598 for eight days to high density in the presence of 1.2. mM Ca^{2+} and treated either with DMSO
599 or 10 µM SRPIN340 dissolved in DMSO for 48 hours. RNA quantification and quality was
600 assessed by Qubit and Agilent TapeStation, respectively. Ribosomal RNA was depleted using
601 the Illumina RiboZero Gold H/M/R Kit (Illumina, UK). Libraries were prepared using the TruSeq
602 Stranded mRNA Kit (Illumina, UK) and cDNA was made using a Superscript II reverse
603 transcriptase reaction (Invitrogen, UK). cDNA was converted to dsDNA and cleaned up using
604 Beckman Coulter's RNAClean XP (1.8 ratio) and then A-tailed. Illumina TruSeq LT adapters
605 were ligated to the samples and cleaned up with a 1:1 bead ratio of AMPure XP followed by
606 size selection using SPRIselect (Beckman Coulter, UK). The library was assessed for quality
607 by Qubit and Agilent TapeStation. RNA paired-end sequencing was carried out using Illumina
608 Genome Analyzer sequencing at the University of Glasgow.
609

610 Alignment of fastq files and read summarization

611 The six raw RNA sequencing fastq files (3 x SRPIN340-treated and 3 x DMSO-treated) were
612 analysed for quality using FastQC (version 0.11.2) and reads were trimmed of adaptor
613 sequences and low-quality bases using Trimgalore. The trimmed reads were aligned to the
614 human genome GRCh38 (*Ensembl*) using Hisat2 (version 2.0.5) [55] in the Linux environment

615 (version 18.04.3). FeatureCounts (Version 1.5.1) [56] was used to quantify the reads by read
616 summarization.
617
618 Differential gene expression analysis
619 Differential gene expression analysis of SRPIN340-treated and DMSO-treated NIKS16 cells
620 was determined using the Bioconductor package (Version 3.12) and DESeq2 (Version 1.30.1)
621 [57], in the R environment (version 4.0.5). Differentially expressed genes were filtered by Q-
622 value<0.05 and log fold change cut off of 2 except for comparison of SRPIN340-related versus
623 HPV16 infection-related changes to NIKS16 gene expression where log fold change of 1.5
624 was used. Genes which were differentially expressed were variance stabilisation transformed
625 for normalisation and visualisation on a heatmap. Pheatmap (version 1.0.12) was used for
626 visualisation.
627
Pathway Analysis
628 BiomaRt (version as 2.46.3) was used to convert *ensembl* gene ID into gene symbols before
629 pathway analysis was performed. Over representation analysis was performed using
630 ClusterProfiler (version 3.18.1) [58] in the R environment. Enrichment of gene ontology (GO)
631 terms was determined for the subontology category, biological processes for 354 up and 241
632 down regulated genes (log fold change >2). The statistical test used includes a
633 hypergeometric statistical test with Bonferroni correction. The thresholds used were Q-value
634 < 0.05. Functional clustering of GO terms was performed using enrichplot (version 1.12.0).
635
636 Comparison of differentially expressed genes upon HPV16 infection
637 Differentially expressed genes from HPV16-infected NIKS16 cells and uninfected NIKS cells
638 [35] were compared manually to differentially expressed genes upon SRPIN340 treatment.
639 Genes involved in epithelial barrier function and innate immunity were identified from both
640 data sets.
641

642

643

644 Over representation analysis of alternative splicing events.

645 Bam files from the RNA paired-end sequencing of 10 μM SRPIN340-treated or DMSO-treated
646 NIKS16 cells were sorted by co-ordinate, indexed and subject to SplAdder analysis [59] to
647 measure and quantify alternative splicing events. Percentage spliced in (PSI) values were
648 quantified for each splicing event and an independent two-tailed students t-test was performed
649 for DMSO-treated and SRPIN340-treated values in order to determine the most significant
650 differentially spliced genes upon SRPIN340 treatment. Pathway analysis was performed using
651 Webgestalt ((http://www.webgestalt.org/) [39]. Over representation analysis was carried out
652 testing for biological processes using Benjamini-Hochberg multiple testing adjustment.

653

654 **ACKNOWLEDGEMENTS**

655 We would like to thank Prof. John Doorbar, University of Cambridge, UK, for providing NIKS
656 and NIKS16 cells lines and the anti-E4 B11 antibody. The sheep anti-E2 antibody was a kind
657 gift from Prof. Joanna Parish, University of Birmingham, UK. Our thanks go to Dr Jean Quinn,
658 University of Glasgow, for 3D raft culture training.

659

660 **DATA AVAILABILITY STATEMENT**

661 The raw data for the results described here is available upon request. RNA-Seq data sets are
662 freely available from the European Nucleotide Archive accession number PRJEB80489.

663

664 **FUNDING**

This work was funded by a studentship #K1513 to AAA Faizo from the King Abdulaziz University, Jeddah, Saudi Arabia. QG is funded by the Medical Research Council grant number MC_UU_00034/5.

AUTHOR CONTRIBUTIONS

AAA. Faizo: Investigation, formal analysis, validation and visualization, writing review and editing.

C. Bellward: Investigation, formal analysis, validation and visualization.

H. Hernandez Lopez: Investigation, formal analysis, validation and visualization, writing review and editing.

A. Stevenson: methodology, supervision, project administration.

Gu Q.: Investigation, formal analysis, supervision, writing review and editing.

S. Graham: Conceptualization, supervision, writing, review and editing

CONFLICT OF INTEREST STATEMENT

We declare no conflict of interest.

681 **FIGURE LEGENDS**

682 **Figure 1. SRPIN340 inhibits phosphorylation of SRSF1 and SRSF3.** NIKS16 cells in
683 monolayer culture were mock-treated or treated with 10 μM SRPIN340 or with the drug
684 vehicle, DMSO. A. Representative western blot and graph of the quantification of levels of
685 SRSF1 relative to levels of β-tubulin. B. Representative western blot and graph of the
686 quantification of levels of SRSF2 relative to levels of β-tubulin. C. Representative western blot
687 and graph of the quantification of levels of SRSF3 relative to levels of β-tubulin. The data
688 shown are the mean and standard deviation from the mean from three separate experiments.
689 $p<0.05$, p-value less than 0.05. *, statistically significant difference in relative protein levels.
690 ns, not statistically significant. D-F. NIKS16 cells treated with DMSO or with 10 μM SRPIN340
691 D. Immunofluorescence microscopy of cells stained with an antibody against SRSF1. E.
692 Immunofluorescence microscopy of cells stained with an antibody against SRSF2. F.
693 Immunofluorescence microscopy of cells stained with an antibody against SRSF3. The left-
694 hand panels show SRSF staining in green. The right-hand panels show SRSF staining merged
695 with DAPI (blue staining). Representative images from three separate experiments are shown.
696 Size bars = 10μm.

697

698 **Figure 2. SRPK1 inhibition does not alter HPV16 oncoprotein expression or activity. A.**
699 Diagram of the E6E7 coding region of the HPV genome showing the unspliced (E6fl) and three
700 spliced RNAs that are transcribed from the region (E6*I, E6*II, E6*X). P_{97}, HPV16 early
701 promoter located at nucleotide 97 on the genome. Forward and reverse facing chevrons
702 indicate the approximate position of the primers used in the PCR reaction in (B). B. Gel image
703 showing end point RT-PCR products using the primers indicated in (A) to amplify all four E6E7
704 mRNAs from NIKS16 cells grown in monolayer culture and treated with DMSO or 10 μM
705 SRPIN340. M = size marker. Western blot of levels of (C) E6 and (E) E7 in monolayer cultured
706 NIKS16 cells either mock-treated or treated with DMSO, or SRPIN340 at 10 μM or 50 μM.
707 HeLa cell extract was included on the blot as a positive control for detection of E6. The upper

708 portion of the blot was reacted with an anti β-tubulin antibody as a loading control. Graph
709 showing quantification of three separate western blot experiments of the levels of (D) E6 and
710 (F) E7 relative to β-tubulin, in HeLa cells as a control and in NIKS16 cells using the various
711 experimental conditions in the western blots. G. Western blots of levels of Rb, p53 and GAPDH
712 as a loading control, in monolayer cultured NIKS16 cells mock-treated or treated with DMSO,
713 or SRPIN340 at 10 μM or 50 μM. H. Graph showing quantification of p53 and Rb levels in the
714 western blot in G. Expression levels were calculated relative to the GAPDH loading control.
715 The data in all the graphs are the mean and standard deviation from the mean from three
716 separate experiments. ns, not statistically significant.

717

718 **Figure 3. SRPK1 inhibition leads to loss of E2 expression through loss of the spliced**
719 **mRNA encoding E2.** A. Diagram of the early region of the HPV16 genome downstream of
720 the E6E7 gene region. P_{670}, HPV16 late promoter located at nucleotide 670 in the E7 coding
721 region. p(A)E, the HPV16 early polyadenylation site. Open rectangles, HPV16 early genes
722 E1, E2, E4, E5. Below is the genome map is shown a diagram of the major spliced mRNA
723 encoding E2. Shaded rectangles, open reading frames. Lines represent RNA sequences
724 which are spliced out to form the E2 mRNA. AAAn, poly(A) tail. Chevrons indicate forward and
725 reverse primers used in the first round of the nested RT-PCR reaction shown in B. A red split
726 chevron indicates the forward primer used in the second round of the nested PCR amplification
727 shown in B**.** This cross-splice epitope primer was used with the reverse primer located inside
728 the E2 open reading frame. SD880, splice donor site at nucleotide 880. SA2709, splice
729 acceptor site at nucleotide 2709. B. Upper panel: ethidium bromide-stained gel showing the
730 products of an RT-PCR reaction to amplify the E2 mRNA from NIKS16 cells cultured in
731 monolayer and treated with DMSO (lane 1) or with SRPIN349 (lane 2), which does not inhibit
732 SRPK1, or with SRPIN340 (lane 3). Lower panel: GAPDH cDNA was amplified as a loading
733 control. The gel picture is split because the GAPDH reactions were electrophoresed on the
734 right-hand side of the same gel used to visualise the E2 amplification products which were

735 electrophoresed on the left-hand side adjacent to the size markers. C. Western blot showing
736 levels of E2 in monolayer cultured and differentiated NIKS16 cells mock-treated, DMSO-
737 treated or treated with either 10 μM or 50 μM SRPIN340. Protein extract from HPV-negative
738 NIKS cell was included in the experiment to demonstrate specificity of the E2 antibody. The
739 upper portion of the blot was reacted with an anti-involucrin antibody to demonstrate that the
740 cells were differentiated. β-tubulin was used as a loading control. D. Graph showing
741 quantification of E2 levels relative to the β-tubulin loading controls in the various experimental
742 conditions used in the western blot in C. The data shown are the mean and standard deviation
743 from the mean from quantification of three separate western blot experiments. $p<0.05$*, p-
744 value indicating a significant difference in E2 expression levels. E. Graph showing
745 quantification of E2 levels relative to the β-tubulin loading controls using protein extracts from
746 NIKS16 cells grown in 3D raft cultures. The data shown are the mean and standard deviation
747 from the mean from three separate western blot experiments Representative western blots
748 showing E2 and β-tubulin levels are shown above the graph. $p<0.05$*, p-value indicating a
749 significant difference in E2 expression levels. F. Immunofluorescence staining with an E2
750 antibody (green staining, left hand panels) and counterstained with DAPI (blue staining, right
751 hand panels) of sections of 3D NIKS16 raft tissues topically treated with DMSO or with 10 μM
752 SPRIN340. Dotted lines indicate the basal membrane of the tissues. Size bars=50 μm.

753

754 **Figure 4. SRPK1 activity is required for HPV16 late gene expression.** A. Western blot
755 analysis of levels of L1 protein in monolayer cultured NIKS16 cells mock-treated or DMSO-
756 treated or treated with 10 μM or 50 μM SRPIN340. NIKS cell extract was included on the blot
757 as a control for the specificity of the L1 antibody. The upper portion of the blot was reacted
758 with an antibody against involucrin to demonstrate that the cells were differentiated. GAPDH
759 was used as a loading control. B. Graph showing quantification of L1 levels relative to the
760 GAPDH loading controls in the various experimental conditions used in the western blot in A.
761 The data shown are the mean and standard deviation from the mean from three separate

762 western blot experiments. p<0.05*, p-value indicating a significant difference in L1 expression
763 levels. C. Western blot analysis of levels of L1 protein in 3D raft cultured NIKS16 tissues
764 topically-treated with either DMSO or 10 μM SRPIN340. NIKS tissue extract was included on
765 the blot as a control for the specificity of the L1 antibody. GAPDH was used as a loading
766 control. D. Graph showing quantification of L1 levels relative to the GAPDH loading control in
767 the experimental conditions used in the western blot in C. The data shown are the mean and
768 standard deviation from the mean from three separate western blot experiments. p<0.05*, p-
769 value indicating a significant difference in L1 expression levels. E. Immunofluorescence
770 microscopy of sections of NIKS16 3D raft tissues topically-treated with DMSO or with 10 μM
771 SRPIN340 and stained with an antibody against E4 (green staining, left-hand panels) or
772 counterstained with DAPI (blue staining, right-hand panels). F. Immunofluorescence
773 microscopy of sections of NIKS16 3D rafts tissues treated with DMSO or treated with 10 μM
774 SRPIN340 and stained with an antibody against L1 (green staining, left-hand panels) or
775 counterstained with DAPI (blue staining, right-hand panels). Dotted lines indicate the basal
776 membrane of the tissues. Size bars=50 μm.

777

778 **Figure 5. RNA sequencing of SRPIN340-treated tissues reveals that the drug**
779 **counteracts some of the effects of HPV16 infection on keratinocytes.** A. Heatmap of
780 overall changes in gene expression in NIKS16 cells caused by SRPIN340 treatment. Three
781 replicates of DMSO-treated and 10 μM SRPIN340-treated NIKS16 cells were sequenced. B.
782 Pie chart showing the relative percentages of categories of SRPIN340 up-regulated genes in
783 NIKS16 cells. The GO terms for the up-regulated pathways are shown on the right-hand side.
784 C. Pie chart showing the relative percentages of categories of SRPIN340 down-regulated
785 genes in NIKS16 cells. The GO terms for the down-regulated pathways are shown on the
786 right-hand side. D. Graph showing genes involved in the epithelial structural barrier that are
787 down-regulated by HPV16 infection [35] but up-regulated by SRPIN340 treatment. E. Graph
788 showing genes involved in innate immunity that are oppositely regulated by HPV16 infection

789 [35] and SRPIN340 treatment. F. Over representation analysis showing the various cellular
790 processes that are altered by SRPIN340-induced changes in alternative splicing.

791

792 **Figure 6. SRPIN340 treatment does not alter cell proliferation or viability in monolayer**
793 **cultured keratinocytes.** A. Proliferation of HPV-negative NIKS cells over 72 hours, mock-
794 treated or following treatment with the drug vehicle DMSO or with 10 μM or 50 μM SRPIN340.
795 B. Proliferation of NIKS16 cells over 72 hours, mock-treated or following treatment with the
796 drug vehicle DMSO or with 10 μM or 50 μM SRPIN340. C. Viability of HPV-negative NIKS
797 cells over 72 hours, mock-treated or following treatment with the drug vehicle DMSO or with
798 10 μM or 50 μM SRPIN340. D. Viability of NIKS16 cells over 72 hours, mock-treated or
799 following treatment with the drug vehicle DMSO or with 10 μM or 50 μM SRPIN340. $p<0.05$,
800 p=value of significance. E. Western blot analysis of levels of MCM2 and Ki67 in NIKS cells
801 mock-treated or following treatment with the drug vehicle DMSO or with 10 μM or 50 μM
802 SRPIN340 for 48 hours. GAPDH was used a loading control. F. Graph of quantification of
803 levels of MCM2 and Ki67 relative to GAPDH in western blots of NIKS cell extracts. The data
804 shown are the mean and standard deviation from the mean from three separate western blot
805 experiments. ns, no significant difference. G. Western blot analysis of levels of MCM2 and
806 Ki67 in NIKS16 cells mock-treated or following treatment with the drug vehicle DMSO or with
807 10 μM or 50 μM SRPIN340 for 48 hours. GAPDH was used a loading control. H. Graph of
808 quantification of levels of MCM2 and Ki67 relative to GAPDH in western blots of NIKS16 cell
809 extracts. The data shown are the mean and standard deviation from the mean from three
810 separate western blot experiments. ns, no significant difference.

811

812 **Supplementary Figure 1. NIKS16 cells contain episomal genomes and undergo late**
813 **events in the viral life cycle.** A. Southern blot analysis of HPV16 genomes in NIKS16 cells.
814 DNA was isolated from monolayer cultured NIKS16 cells and digested with either Bam HI,

815 which cuts the genome once (lane 2), or Hind III, which does not cut the genome (lane 3). The
816 HPV16 genome was cut from plasmid pEF-HPV16 with Bam HI as a size control for the
817 episomal genome (lane 1). B. Western blot analysis of HPV16 E2 and L1 expression in protein
818 lysates from NIKS and NIKS16 cells grown in monolayer culture to give an undifferentiated
819 cell population (U, lanes 1 & 2) or differentiated by growing to high density in the presence of
820 1.2 mM Ca^{2+} (D, lanes 3 & 4). Involucrin and keratin 10 were used as controls for keratinocyte
821 differentiation. GADPH is used as a loading control.

822

823 **Supplementary Figure 2. Topical SRPIN340 treatment of 3D raft tissues does not disrupt**
824 **tissue morphology and may be transmitted throughout the tissues.** A. H&E staining of
825 NIKS16 3D raft tissues grown for 12 days then grown in the presence of 10 or 50 μM
826 SRPIN340 in the culture medium for 48 hours. B. H&E staining of NIKS16 3D raft tissues
827 grown for 12 days followed by topical application of 10 or 50 μM SRPIN340 in a 50 μl droplet
828 and incubation for 48 hours. C. Autofluorescence control of NIKS16 3D tissues stained with
829 the same secondary antibody used in D. D. Immunofluorescence microscopy of NIKS16 3D
830 tissues topically treated with Alexa-fluor 488 (Alexa488: green staining). Tissues in the right-
831 hand panels of C. and D. are counterstained with DAPI. The junction of the basal layer of cells
832 with the dermal equivalent is indicated by a dotted line. Size bars = 50 μM.

833

834 **Supplementary Figure 3. SRPIN340 treatment does not alter expression of the HPV16**
835 **major late mRNAs.** A. Diagram of the portion of the HPV16 genome downstream of the P_{670}
836 promoter. The E1^E4^L1 alternatively spliced mRNA that encodes E4 and L1 and the
837 readthrough mRNA E1^E4, E5, L2 and L1 that is thought to encode L2 are shown beloiw the
838 genome map. P_{670}, HPV16 late promoter located at nucleotide 670. p(A)L, late polyadenylation
839 site. Open rectangles, HPV16 genes E1, E2, E4, E5, L2 and L1. Shaded rectangles, open
840 reading frames. Lines represent RNA sequences which are spliced out to form the mRNAs.

841 AAAn, poly(A) tail. Chevrons indicate the approximate positions of forward and reverse
842 primers used in the PCR reactions shown in (B) and (C). B. Ethidium bromide-stained gel
843 showing the PCR products obtained from amplification of NIKS16 cDNA using the primer pair
844 indicated in (A) for the E1^E4^L1 mRNA. GAPDH primer pairs were added to the same
845 reaction for a loading control. * non-specific bands. C. Upper panel: ethidium bromide-stained
846 gel showing the PCR products obtained from amplification of NIKS16 cDNA using the primer
847 pairs indicated in (A) in a nested PCR reaction to amplify across the L2-L1 junction from the
848 E1^E4, E5, L2, L1 readthrough mRNA. Lower panel: amplification of GAPDH as a loading
849 control. In (B) and (C) the gel pictures are split because additional reactions were
850 electrophoresed between the marker lane and the DMSO and SRPIN340 lanes.

851

852

	Sample	No. of reads	Alignment to HPV16 genome (%)	Alignment to Human Genome (%)
No drug	1	46578063	0.04	82.10
No drug	2	29538705	0.04	85.16
No drug	3	37758387	0.04	80.54
SRPIN340	4	28468475	0.05	84.32
SRPIN340	5	31260092	0.05	86.22
SRPIN340	6	32025480	0.04	80.28

853

854 **Table 1**. Number of sequencing reads and percent alignment to the HPV16 and human
855 genomes for each sample subjected to RNA sequencing.

Gene	Negative fold change	Positive fold change	Q-value
TMPRSS11D		6.797647766	8.66E-05
SERPINB11		6.032431007	0.000679
CYP1A1		5.968312781	1.21E-25
HRNR		5.415118392	0.004903
ENDOU		4.90915265	1.9E-06
LOR		4.607461151	0.001384
FAIM2		4.555164059	0.010715
LIPN		4.437793821	0.017848
SH2D1B		4.393057631	2.56E-05
CRNN		4.163890496	6.37E-29
CAPN14		4.084787111	1.06E-05
AQP5		4.069593091	6.13E-19
KLK12		4.00172104	4.12E-13
TMPRSS11A		3.98695018	3.71E-15
FLG2		3.887629517	9.25E-17
CEACAM5		3.819780979	0.000152
S100A7		6.797647766	8.66E-05
ARG1		6.032431007	0.000679
SPINK7		3.463702469	1.75E-31
SPAG17		3.4159458	8.97E-05
ANKRD1	-4.307959272		0.000146
MYL9	-4.205082349		6.30E-05
MYL7	-3.538350233		2.91E-06
GLP2R	-3.287298644		0.021162

MGP	-2.883346003		5.85E-19
KDR	-2.856988802		3.51E-24
ALDH1L2	-2.742967901		0.000597
TGM2	-2.707864354		4.79E-17
DRD2	-2.678088804		0.007043
ALOX5AP	-2.67413198		6.89E-06
TAGLN	-2.544919939		5.02E-34
COL8A1	-2.329975942		1.59E-12
SELENOP	-2.313804905		0.035668
TOX2	-2.279567504		0.035591
WFDC2	-2.742967901		0.000102
SLC7A7	-2.087552302		6.50E-05
ANPEP	-1.964638827		0.003945
C3	-1.951676084		1.11E-30
PTPRB	-1.933491109		0.00429349
SLCO2A1	-1.915283426		1.33E-03

Table 2. Fold change of the top 20 up- and 20 down-regulated protein-coding genes by SRPIN340 treatment compared to DMSO treatment in NIKS16 cells. Q-value adjusted for multiple hypotheses by DESeq2 analysis.

865 **REFERENCES**

866

867 1. Egawa N, Egawa K, Griffin H, Doorbar J. Human Papillomaviruses; Epithelial
868 Tropisms, and the Development of Neoplasia. Viruses. 2015;7(7):2802. PubMed PMID:
869 doi:10.3390/v7072802.
870 2. Stanley MA. Epithelial Cell Responses to Infection with Human Papillomavirus. Clin
871 Microbiol Rev. 2012;25(2):215-22. doi: 10.1128/cmr.05028-11.
872 3. Graham SV. The human papillomavirus replication cycle, and its links to cancer
873 progression: a comprehensive review. Clin Sci (Lond). 2017;131(17):2201-21. Epub
874 20170810. doi: 10.1042/cs20160786.
875 4. Harper DM, DeMars LR. HPV vaccines – A review of the first decade. Gynecol
876 Oncol. 2017;146(1):196-204. doi: 10.1016/j.ygyno.2017.04.004.
877 5. Kirk A, Graham SV. The human papillomavirus late life cycle and links to
878 keratinocyte differentiation. J Med Virol. 2024;96(2):e29461. doi: 10.1002/jmv.29461.
879 6. McBride AA. Human papillomaviruses: diversity, infection and host interactions. Nat
880 Rev Microbiol. 2022;20(2):95-108. Epub 20210914. doi: 10.1038/s41579-021-00617-5.
881 7. Vande Pol SB, Klingelhutz AJ. Papillomavirus E6 oncoproteins. Virology.
882 2013;445(1–2):115-37. doi: 10.1016/j.virol.2013.04.026.
883 8. Roman A, Munger K. The papillomavirus E7 proteins. Virology. 2013;445(1):138-68.
884 doi: 10.1016/j.virol.2013.04.013.
885 9. Egawa N, Wang Q, Griffin HM, Murakami I, Jackson D, Mahmood R, Doorbar J.
886 HPV16 and 18 genome amplification show different E4-dependence, with 16E4 enhancing
887 E1 nuclear accumulation and replicative efficiency via its cell cycle arrest and kinase
888 activation functions. PLOS Pathogens. 2017;13(3):e1006282. doi:
889 10.1371/journal.ppat.1006282.
890 10. Zhou Z, Fu X-D. Regulation of splicing by SR proteins and SR protein-specific
891 kinases. Chromosoma. 2013;122(3):191-207. doi: 10.1007/s00412-013-0407-z.

892 11. Long JC, Caceres JF. The SR protein family of splicing factors: master regulators of
893 gene expression. Biochem J. 2009;417(1):15-27.
894 12. Giannakouros T, Nikolakaki E, Mylonis I, Georgatsou E. Serine-arginine protein
895 kinases: a small protein kinase family with a large cellular presence. FEBS J.
896 2011;278(4):570-86. doi: 10.1111/j.1742-4658.2010.07987.x.
897 13. Aubol BE, Wu G, Keshwani MM, Movassat M, Fattet L, Hertel KJ, et al. Release of
898 SR Proteins from CLK1 by SRPK1: A Symbiotic Kinase System for Phosphorylation Control
899 of Pre-mRNA Splicing. Mol Cell. 2016;63(2):218-28. Epub 20160707. doi:
900 10.1016/j.molcel.2016.05.034.
901 14. Yun CY, Fu XD. Conserved SR protein kinase functions in nuclear import and its
902 action is counteracted by arginine methylation in Saccharomyces cerevisiae. J Cell Biol.
903 2000;150(4):707-18. doi: 10.1083/jcb.150.4.707.
904 15. Lai MC, Lin RI, Huang SY, Tsai CW, Tarn WY. A human importin-beta family protein,
905 transportin-SR2, interacts with the phosphorylated RS domain of SR proteins. J Biol Chem.
906 2000;275(11):7950-7. doi: 10.1074/jbc.275.11.7950.
907 16. Nikolakaki E, Sigala I, Giannakouros T. Good Cop, Bad Cop: The Different Roles of
908 SRPKs. Front Genet. 2022;13:902718. Epub 20220602. doi: 10.3389/fgene.2022.902718.
909 17. Graham SV. Human papillomavirus: gene expression, regulation and prospects for
910 novel diagnostic methods and antiviral therapies. Future Microbiol. 2010;5(10):1493-505.
911 18. Yu L, Majerciak V, Zheng ZM. HPV16 and HPV18 Genome Structure, Expression,
912 and Post-Transcriptional Regulation. Int J Mol Sci. 2022;23(9). Epub 20220429. doi:
913 10.3390/ijms23094943.
914 19. Klymenko T, Hernandez-Lopez H, MacDonald AI, Bodily JM, Graham SV. Human
915 papillomavirus E2 regulates SRSF3 (SRp20) to promote capsid protein expression in
916 infected differentiated keratinocytes. J Virol. 2016. doi: 10.1128/jvi.03073-15.
917 20. Mole S, Faizo AAA, Hernandez-Lopez H, Griffiths M, Stevenson A, Roberts S,
918 Graham SV. Human papillomavirus type 16 infection activates the host serine arginine

919 protein kinase 1 (SRPK1) - splicing factor axis. J Gen Virol. 2020;101(5):523-32. Epub
920 20200313. doi: 10.1099/jgv.0.001402.
921 21. Bodaghi S, Jia R, Zheng Z-M. Human papillomavirus type 16 E2 and E6 are RNA-
922 binding proteins and inhibit in vitro splicing of pre-mRNAs with suboptimal splice sites.
923 Virology. 2009;386(1):32-43. doi: 10.1016/j.virol.2008.12.037.
924 22. Oltean S, Gammons M, Hulse R, Hamdollah-Zadeh M, Mavrou A, Donaldson L, et al.
925 SRPK1 inhibition in vivo: modulation of VEGF splicing and potential treatment for multiple
926 diseases. Biochem Soc Trans. 2012;40(4):831-5. doi: 10.1042/bst20120051.
927 23. Bates DO, Morris JC, Oltean S, Donaldson LF. Pharmacology of Modulators of
928 Alternative Splicing. Pharmacol Rev. 2017;69(1):63-79. doi: 10.1124/pr.115.011239.
929 24. Karakama Y, Sakamoto N, Itsui Y, Nakagawa M, Tasaka-Fujita M, Nishimura-
930 Sakurai Y, et al. Inhibition of hepatitis C virus replication by a specific inhibitor of serine-
931 arginine-rich protein kinase. Antimicrob Agents Chemother. 2010;54(8):3179-86. Epub
932 20100524. doi: 10.1128/aac.00113-10.
933 25. Fukuhara T, Hosoya T, Shimizu S, Sumi K, Oshiro T, Yoshinaka Y, et al. Utilization
934 of host SR protein kinases and RNA-splicing machinery during viral replication. Proc Natl
935 Acad Sci U S A. 2006;103(30):11329-33. Epub 20060713. doi: 10.1073/pnas.0604616103.
936 26. Sciabica KS, Dai QJ, Sandri-Goldin RM. ICP27 interacts with SRPK1 to mediate
937 HSV splicing inhibition by altering SR protein phosphorylation. EMBO J. 2003;22(7):1608-
938 19.
939 27. Daub H, Blencke S, Habenberger P, Kurtenbach A, Dennenmoser J, Wissing J, et al.
940 Identification of SRPK1 and SRPK2 as the major cellular protein kinases phosphorylating
941 hepatitis B virus core protein. J Virol. 2002;76(16):8124-37. doi: 10.1128/jvi.76.16.8124-
942 8137.2002.
943 28. Kajitani N, Schwartz S. The role of RNA-binding proteins in the processing of mRNAs
944 produced by carcinogenic papillomaviruses. Semin Cancer Biol. 2022;86(Pt 3):482-96. Epub
945 20220216. doi: 10.1016/j.semcancer.2022.02.014.

946 29. Graham SV. HPV and RNA Binding Proteins: What We Know and What Remains to
947 Be Discovered. Viruses. 2024;16(5). Epub 20240515. doi: 10.3390/v16050783.
948 30. Weschler EI, Wang Q, Roberts I, Pagliarulo E, Jackson D, Untersperger C, et al.
949 Reconstruction of human papillomavirus type 16-mediated early-stage neoplasia implicated
950 E6/E7 deeregualtion and the loss of contact inhibition in neoplastic progression. J Virol.
951 2012;86(11):6358-64.
952 31. Flores ER, Allen-Hoffmann BL, Lee D, Sattler CA, Lambert PF. Establishment of the
953 human papillomavirus type 16 (HPV-16) life cycle in an immortalized human foreskin
954 keratinocyte cell line. Virology. 1999;262. doi: 10.1006/viro.1999.9868.
955 32. Weber PA, Chang HC, Spaeth KE, Nitsche JM, Nicholson BJ. The permeability of
956 gap junction channels to probes of different size is dependent on connexin composition and
957 permeant-pore affinities. Biophys J. 2004;87(2):958-73. doi: 10.1529/biophysj.103.036350.
958 33. Zheng Y, Cui X, Nilsson K, Yu H, Gong L, Wu C, Schwartz S. Efficient production of
959 HPV16 E2 protein from HPV16 late mRNAs spliced from SD880 to SA2709. Virus Res.
960 2020;285:198004. Epub 20200505. doi: 10.1016/j.virusres.2020.198004.
961 34. Evans MR, James CD, Bristol ML, Nulton TJ, Wang X, Kaur N, et al. Human
962 Papillomavirus 16 E2 Regulates Keratinocyte Gene Expression Relevant to Cancer and the
963 Viral Life Cycle. J Virol 2019;93(4):e01941-18. doi: 10.1128/JVI.01941-18 %J.
964 35. Klymenko T, Gu Q, Herbert I, Stevenson A, Iliev V, Watkins G, et al. RNA-Seq
965 Analysis of Differentiated Keratinocytes Reveals a Massive Response to Late Events during
966 Human Papillomavirus 16 Infection, Including Loss of Epithelial Barrier Function. J Virol
967 2017;91(24):e01001-17. doi: 10.1128/JVI.01001-17 %J.
968 36. Matsui T, Amagai M. Dissecting the formation, structure and barrier function of the
969 stratum corneum. Int Immunol. 2015;27(6):269-80. doi: 10.1093/intimm/dxv013.
970 37. Lessard JC, Piña-Paz S, Rotty JD, Hickerson RP, Kaspar RL, Balmain A, Coulombe
971 PA. Keratin 16 regulates innate immunity in response to epidermal barrier breach. Proc Natl
972 Acad Sci U S A. 2013;110(48):19537-42. Epub 20131111. doi: 10.1073/pnas.1309576110.

973 38. Carregaro F, Stefanini ACB, Henrique T, Tajara EH. Study of small proline-rich
974 proteins (SPRRs) in health and disease: a review of the literature. Arch Dermatol Res.
975 2013;305(10):857-66. doi: 10.1007/s00403-013-1415-9.
976 39. Liao Y, Wang J, Jaehnig EJ, Shi Z, Zhang B. WebGestalt 2019: gene set analysis
977 toolkit with revamped UIs and APIs. Nucleic Acids Res. 2019;47(W1):W199-w205. doi:
978 10.1093/nar/gkz401.
979 40. Cartegni L, Wang J, Zhu Z, Zhang MQ, Krainer AR. ESEfinder: A web resource to
980 identify exonic splicing enhancers. Nucleic Acids Res. 2003;31(13):3568-71. doi:
981 10.1093/nar/gkg616.
982 41. Hao C, Zheng Y, Jönsson J, Cui X, Yu H, Wu C, et al. hnRNP G/RBMX enhances
983 HPV16 E2 mRNA splicing through a novel splicing enhancer and inhibits production of
984 spliced E7 oncogene mRNAs. Nucleic Acids Res. 2022;50(7):3867-91. doi:
985 10.1093/nar/gkac213.
986 42. Gauson EJ, Windle B, Donaldson MM, Caffarel MM, Dornan ES, Coleman N, et al.
987 Regulation of human genome expression and RNA splicing by human papillomavirus 16 E2
988 protein. Virology. 2014;468–470:10-8. doi: 10.1016/j.virol.2014.07.022.
989 43. Prescott EL, Brimacombe CL, Hartley M, Bell I, Graham S, Roberts S. Human
990 Papillomavirus Type 1 E1^E4 Protein Is a Potent Inhibitor of the Serine-Arginine (SR)
991 Protein Kinase SRPK1 and Inhibits Phosphorylation of Host SR Proteins and of the Viral
992 Transcription and Replication Regulator E2. J Virol. 2014;88(21):12599-611. doi:
993 10.1128/jvi.02029-14.
994 44. Patel M, Sachidanandan M, Adnan M. Serine arginine protein kinase 1 (SRPK1): a
995 moonlighting protein with theranostic ability in cancer prevention. Mol Biol Rep.
996 2019;46(1):1487-97. Epub 20181208. doi: 10.1007/s11033-018-4545-5.
997 45. Johansson C, Somberg M, Li X, Backström Winquist E, Fay J, Ryan F, et al. HPV-16
998 E2 contributes to induction of HPV-16 late gene expression by inhibiting early
999 polyadenylation. EMBO J. 2012;31(14):3212-27. Epub 20120522. doi:
1000 10.1038/emboj.2012.147.

1001 46. Davy C, McIntosh P, Jackson DJ, Sorathia R, Miell M, Wang Q, et al. A novel
1002 interaction between the human papillomavirus type 16 E2 and E1^E4 proteins leads to
1003 stabilization of E2. Virology. 2009;394(2):266-75. doi: 10.1016/j.virol.2009.08.035.
1004 47. Siddiqa A, Léon KC, James CD, Bhatti MF, Roberts S, Parish JL. The human
1005 papillomavirus type 16 L1 protein directly interacts with E2 and enhances E2-dependent
1006 replication and transcription activation. J Gen Virol. 2015;96(8):2274-85. doi:
1007 doi:10.1099/vir.0.000162.
1008 48. Bazzi H, Christiano AM. Broken hearts, woolly hair, and tattered skin: when
1009 desmosomal adhesion goes awry. Curr Opin Cell Biol. 2007;19(5):515-20.
1010 doi:10.1016/j.ceb.2007.08.001.
1011 49. Morizane S, Sunagawa K, Nomura H, Ouchida M. Aberrant serine protease activities
1012 in atopic dermatitis. J Dermatol Sci. 2022;107(1):2-7. Epub 20220628. doi:
1013 10.1016/j.jdermsci.2022.06.004.
1014 50. Kanno Y, Matsui Y. Cellular coupling in cancerous stomach epithelium. Nature.
1015 1968;218:775-6.
1016 51. Guo T, Zambo KDA, Zamuner FT, Ou T, Hopkins C, Kelley DZ, et al. Chromatin
1017 structure regulates cancer-specific alternative splicing events in primary HPV-related
1018 oropharyngeal squamous cell carcinoma. Epigenetics. 2020;15(9):959-71. Epub 20200322.
1019 doi: 10.1080/15592294.2020.1741757.
1020 52. Kelley DZ, Flam EL, Guo T, Danilova LV, Zamuner FT, Bohrson C, et al. Functional
1021 characterization of alternatively spliced GSN in head and neck squamous cell carcinoma.
1022 Transl Res. 2018;202:109-19. Epub 20180726. doi: 10.1016/j.trsl.2018.07.007.
1023 53. Jeon S, Allen-Hoffman BL, Lambert PF. Integration of human papillomavirus type 16
1024 into the human genome correlates with a selective growth advantage of cells. J Virol.
1025 1995;69(5):2989-97.
1026 54. Anacker D, Moody C. Generation of organotypic raft cultures from primary human
1027 keratinocytes. J Vis Exp. 2012;(60). Epub 20120222. doi: 10.3791/3668.

1028 55. Kim D, Paggi JM, Park C, Bennett C, Salzberg SL. Graph-based genome alignment
1029 and genotyping with HISAT2 and HISAT-genotype. Nat Biotechnol. 2019;37(8):907-15.
1030 Epub 20190802. doi: 10.1038/s41587-019-0201-4.
1031 56. Liao Y, Smyth GK, Shi W. featureCounts: an efficient general purpose program for
1032 assigning sequence reads to genomic features. Bioinformatics. 2014;30(7):923-30. Epub
1033 20131113. doi: 10.1093/bioinformatics/btt656.
1034 57. Love MI, Huber W, Anders S. Moderated estimation of fold change and dispersion for
1035 RNA-seq data with DESeq2. Genome Biol. 2014;15(12):550. doi: 10.1186/s13059-014-
1036 0550-8.
1037 58. Yu G, Wang LG, Han Y, He QY. clusterProfiler: an R package for comparing
1038 biological themes among gene clusters. Omics. 2012;16(5):284-7. Epub 20120328. doi:
1039 10.1089/omi.2011.0118.
1040 59. Kahles A, Ong CS, Zhong Y, Rätsch G. SplAdder: identification, quantification and
1041 testing of alternative splicing events from RNA-Seq data. Bioinformatics. 2016;32(12):1840-
1042 7. Epub 20160211. doi: 10.1093/bioinformatics/btw076.
1043

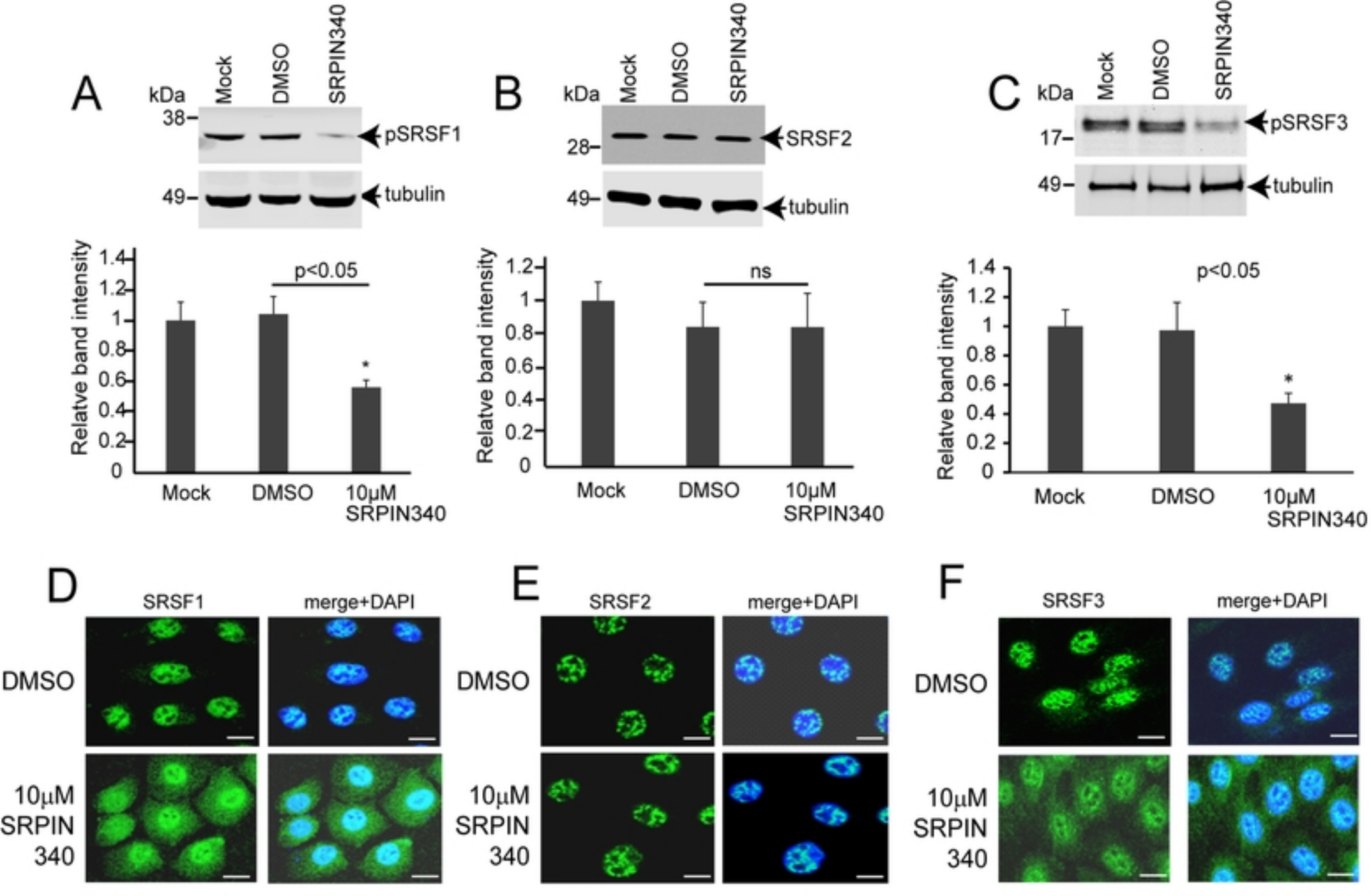
A
kDa
Mock
DMSO
SRPIN340
38
pSRSF1
49
tubulin
Relatve band intensity
p<0.05
Mock
DMSO
10μM SRPIN340
B
kDa
Mock
DMSO
SRPIN340
28
SRSF2
49
tubulin
Relatve band intensity
ns
Mock
DMSO
10μM SRPIN340
C
kDa
Mock
DMSO
SRPIN340
17
pSRSF3
49
tubulin
Relatve band intensity
p<0.05
Mock
DMSO
10μM SRPIN340
D
SRSF1
merge+DAPI
DMSO
10μM SRPIN 340
E
SRSF2
merge+DAPI
DMSO
10μM SRPIN 340
F
SRSF3
merge+DAPI
DMSO
10μM SRPIN 340

Figure1

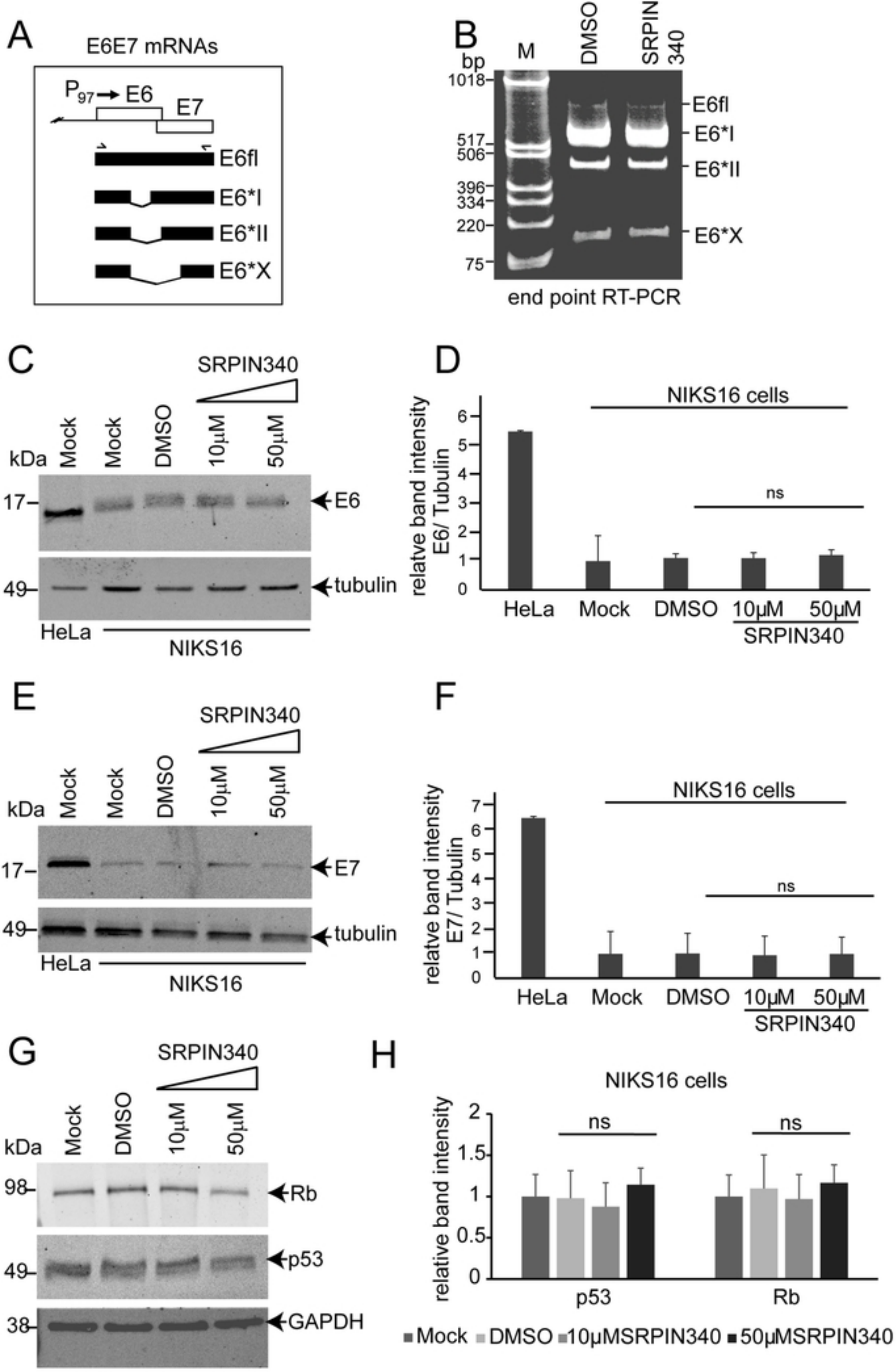

Figure 4 Faizo

Figure2

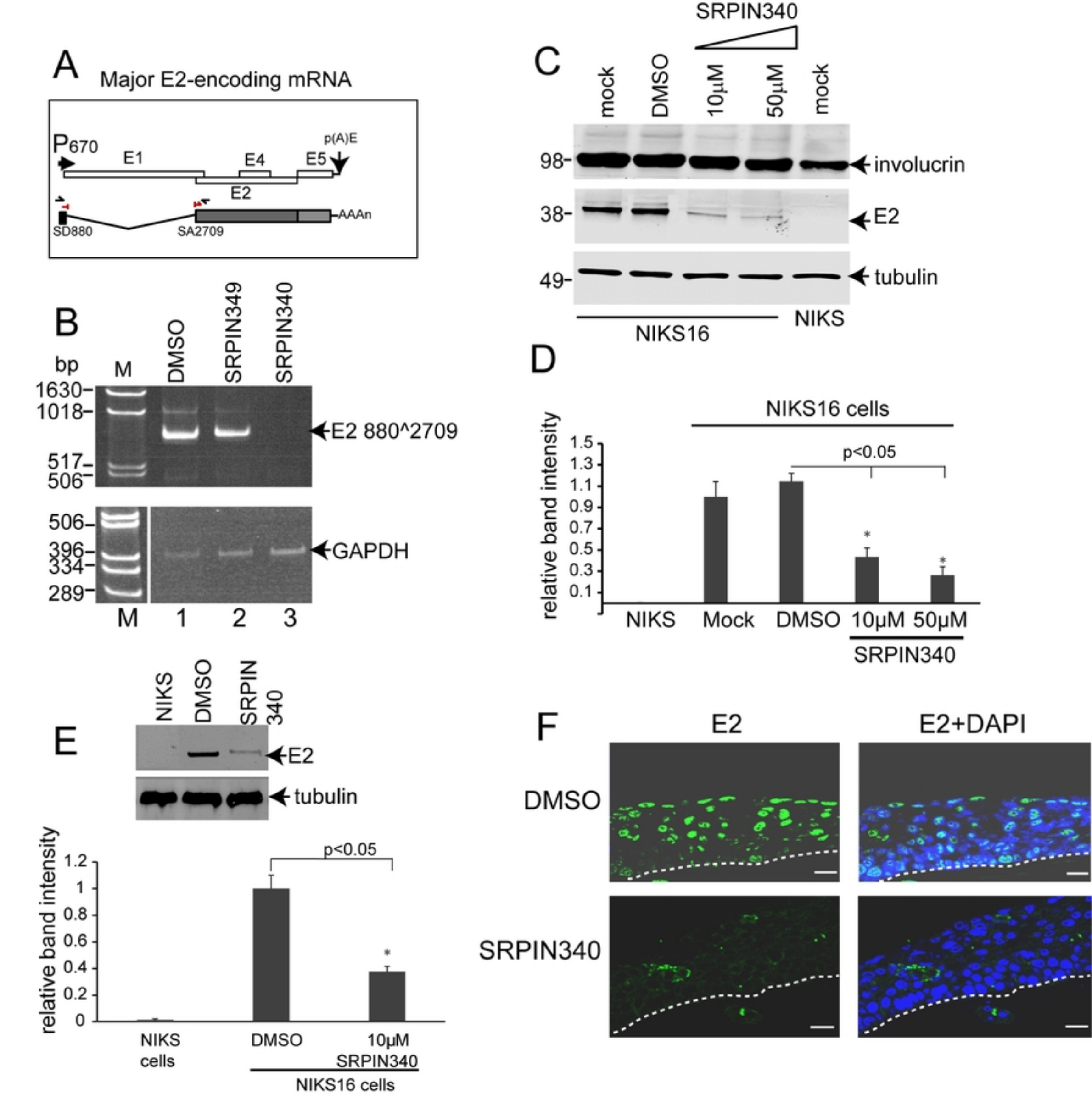
A
Major E2-encoding mRNA
P670
E1
E4
E5
p(A)E
E2
SD880
SA2709
AAAn
B
bp
M
DMSO
SRPIN349
SRPIN340
1630
1018
517
506
E2 880^2709
506
396
334
289
GAPDH
M
1
2
3
C
SRPIN340
mock
DMSO
10μM
50μM
mock
98
38
49
involucrin
E2
tubulin
NIKS16
NIKS
D
NIKS16 cells
relative band intensity
p<0.05
NIKS
Mock
DMSO
10μM
50μM
SRPIN340
E
NIKS
DMSO
SRPIN 340
E2
tubulin
relative band intensity
p<0.05
NIKS cells
DMSO
10μM SRPIN340
NIKS16 cells
F
E2
E2+DAPI
DMSO
SRPIN340

Figure3

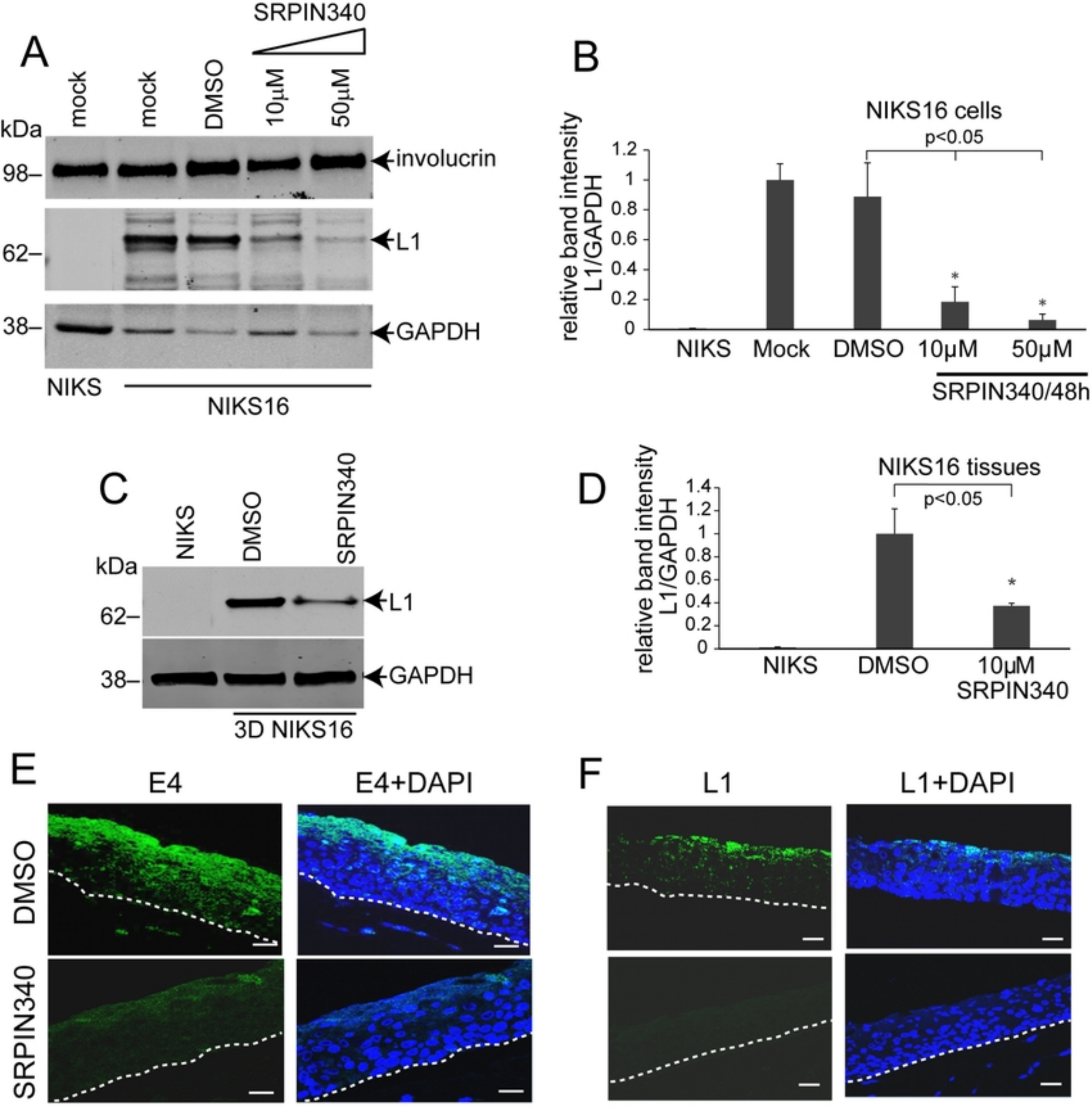

Figure 6 Faizo

Figure4

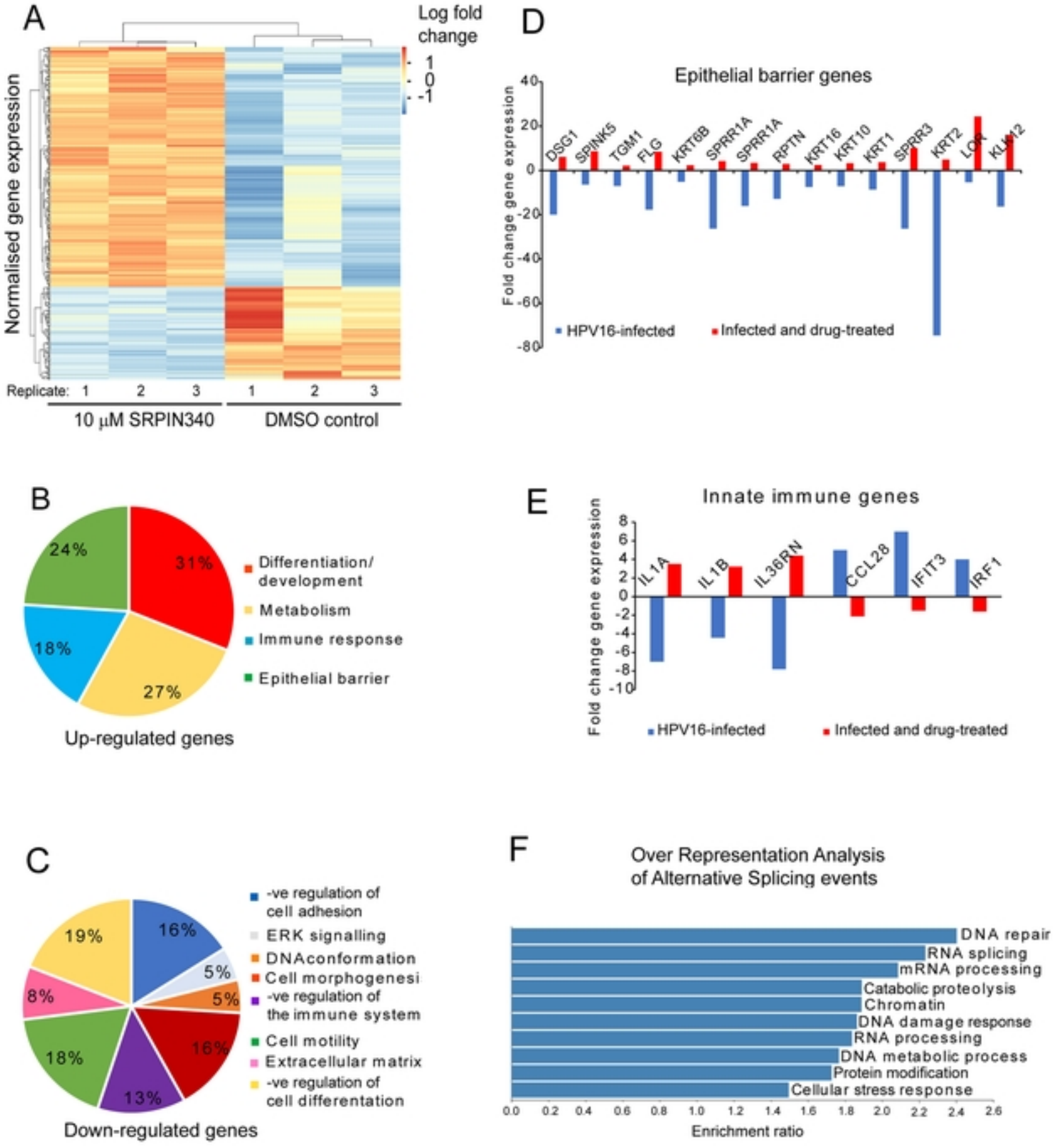
A
Log fold change
1
0
-1
Normalised gene expression
Replicate: 1 2 3 1 2 3
10 μM SRPIN340
DMSO control
D
Epithelial barrier genes
Fold change gene expression
40
20
0
-20
-40
-60
-80
DSG1
SPINK5
TGM1
FLG
KRT6B
SPRR1A
SPRR1A
RPTN
KRT16
KRT10
KRT1
SPRR3
KRT2
LOR
KLK12
HPV16-infected
Infected and drug-treated
B
24%
31%
18%
27%
Differentiation/ development
Metabolism
Immune response
Epithelial barrier
Up-regulated genes
E
Innate immune genes
Fold change gene expression
8
6
4
2
0
-2
-4
-6
-8
-10
IL1A
IL1B
IL36RN
CCL28
IFIT3
IRF1
HPV16-infected
Infected and drug-treated
C
19%
16%
5%
8%
5%
18%
16%
13%
-ve regulation of cell adhesion
ERK signalling
DNAconformation
Cell morphogenesi
-ve regulation of the immune system
Cell motility
Extracellular matrix
-ve regulation of cell differentation
Down-regulated genes
F
Over Representation Analysis of Alternative Splicing events
DNA repair
RNA splicing
mRNA processing
Catabolic proteolysis
Chromatin
DNA damage response
RNA processing
DNA metabolic process
Protein modification
Cellular stress response
0.0 0.2 0.4 0.6 0.8 1.0 1.2 1.4 1.6 1.8 2.0 2.2 2.4 2.6
Enrichment ratio

Figure5

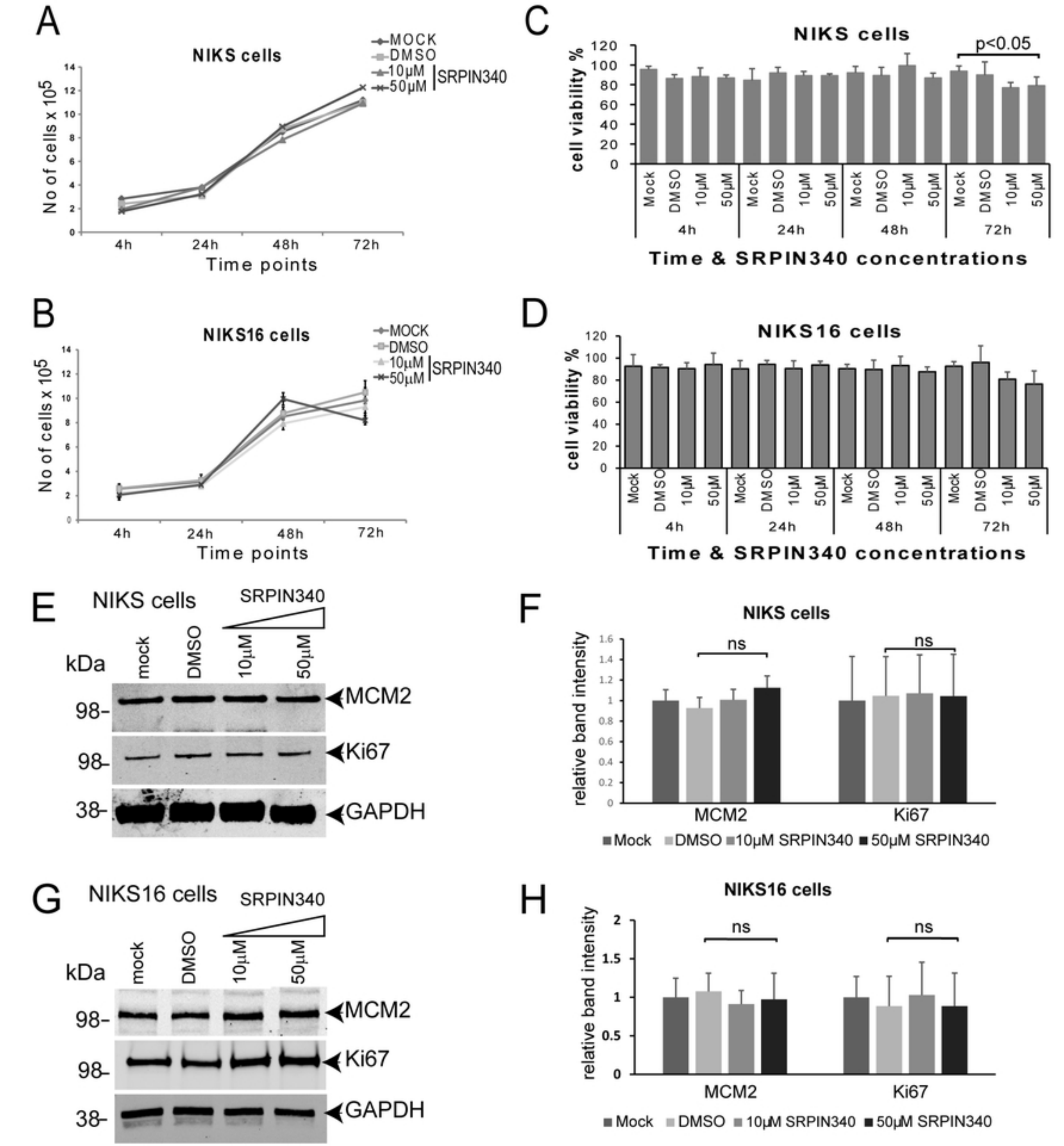
A
NIKS cells
MOCK
DMSO
10μM
50μM
SRPIN340
No of cells x 10^5
4h
24h
48h
72h
Time points
B
NIKS16 cells
MOCK
DMSO
10μM
50μM
SRPIN340
No of cells x 10^5
4h
24h
48h
72h
Time points
C
NIKS cells
p<0.05
cell viability %
Mock
DMSO
10μM
50μM
4h
24h
48h
72h
Time & SRPIN340 concentrations
D
NIKS16 cells
cell viability %
Mock
DMSO
10μM
50μM
4h
24h
48h
72h
Time & SRPIN340 concentrations
E
NIKS cells
SRPIN340
kDa
mock
DMSO
10μM
50μM
98-
MCM2
98-
Ki67
38-
GAPDH
F
NIKS cells
ns
ns
relative band intensity
MCM2
Ki67
Mock
DMSO
10μM SRPIN340
50μM SRPIN340
G
NIKS16 cells
SRPIN340
kDa
mock
DMSO
10μM
50μM
98-
MCM2
98-
Ki67
38-
GAPDH
H
NIKS16 cells
ns
ns
relative band intensity
MCM2
Ki67
Mock
DMSO
10μM SRPIN340
50μM SRPIN340

Figure6